

Final Report

Work Area 3 - Geochemistry

Nov 98 – Dec 99

"SACS" – Saline Aquifer CO₂ Storage

Reporting period: 01/11/98 - 31/12/99
Contract Number: OG / 306 / 98 / NO
Contractor: Den norske stats oljeselskap a.s.

Report compiled by: Isabelle Czernichowski (BRGM)
tel: 33 3 22 91 42 47
fax: 33 3 22 92 31 90
e-mail: i.czernichowski@brgm.fr

Date: 18 december 1999

Authors: Czernichowski-Lauriol I., Sanjuan B., Lanini S., Thiéry D. (BRGM)
Rochelle C.A. (BGS)
Springer N. (GEUS)
Brosse E. (IFP)

Contents

1. Executive summary	2
2. Work carried out during the reporting period	2
3. Problems and difficulties encountered	31
4. Any changes or modifications from the original project	31
5. Compliance with the work programme as outlined in Annex I	32
6. Cost variations from the given original estimate included in the contract	32
7. Patents, if any, applied for or issued during the reporting period	32
8. Brief forecast of the next six month's activities and work	32
9. References	34

1. Executive Summary

The overall objective of this work area is to determine the potential for chemical reactions between the reservoir rock (Utsira sand) and injected CO₂. Work achieved over the reporting period has been:

- (i) the assessment of the initial fluid/rock geochemical state prior to CO₂ injection (Task 3.1),
- (ii) the initiation of laboratory experiments (Task 3.2), and in particular the initiation and initial sampling of long-term batch experiments running under in-situ conditions, development work on flow experiments and analytical methodologies,
- (iii) the development and running tests of geochemical and coupled reaction-transport numerical codes (Task 3.3).

The three tasks of the geochemical programme will continue into SACS II. Work is still underway and the results so far may change.

Part of the originally planned geochemical work within SACS has been shifted to SACS II, due to the opportunity to acquire seismic data in 1999.

The main problem encountered during the reporting period was that of difficulties in obtaining rock and fluid samples, fluid chemical data and mineralogical data. This introduced some delay on the beginning of all tasks of the geochemical work programme, which was partly alleviated by the post-ponement of part of the work on the SACS II project.

The scarcity of geochemical data and sample material at Sleipner is a real concern and could disservice the SACS scientific results when presented to the public, regulatory bodies, and the scientific community. A note has been written about the need to get at least a water sample and a caprock core sample in the Sleipner area, taking advantage of possible future exploratory wells.

2. Work carried out during the reporting period

2.1. PROJECT MANAGEMENT

Steering Committee Meeting ("Kick-off"), Trondheim, NO, 29 October 1998.

Work Meeting, Geological Group, Copenhagen, DK, 9 December. Participants: GEUS, BGS & SINTEF.

Steering Committee Meeting, Sunbury, UK, 17 February 1999.

Work Meeting, Geological Group, Haarlem, NL, 10 March. Participants: NITG-TNO, GEUS, BGS & SINTEF.

Work Meeting, Geochemical Group, Copenhagen, DK, 30 March. Participants: BRGM, BGS & GEUS

Work Meeting, Geological & Geophysical Groups, Copenhagen, DK, 26-28 April. Participants: GEUS, BGS, NITG-TNO & SINTEF

Steering Committee Meeting, Hoofddorp, NL, 7 May.

Steering Committee Meeting, Stavanger, NO, 8 June

Steering Committee Meeting, Stocholm, SU, 23 September

SACS Technical Workshop, Nottingham, UK, 8-9 November

Steering Committee Meeting, Nottingham, UK, 9 November

2.2. DISSEMINATION

No dissemination about the geochemical work.

2.3. NATIONAL, EUROPEAN & INTER-CONTINENTAL CO-OPERATION

a) National

Close contacts with national authorities in NO, DK, NL and UK have been maintained; basically through the research institutes, but also through industry partners. Contact with french national authorities has been sought with Christian Fouillac, Deputy director of the Reseach Division of BRGM.

This is related to efforts to involve the national authorities in Europe early to prepare for common rules for CO₂ injection operations in the underground.

b) EU 5th Framework Programme

- SACS2 : Application for remaining years (2000-2001) and for postponed part of SACS-Thermie work

c) Inter-continental / IEA “Umbrella” Programme

Proposals of geochemical elements for an “umbrella programme” were sent by BRGM and IFP to IEA in March 1999.

Contacts for close co-operation in the geochemical aspects of CO₂ aquifer disposal are being established with the Weyburn project, Canada, and the Battelle institute, US.

2.4. WORK AREAS

WORK AREA 3 – GEOCHEMISTRY

The overall objective of this work area is to determine the potential for chemical reactions between the reservoir rock (Utsira sand) and caprock, and injected CO₂. This is aimed to assess :

- how much CO₂ can be trapped by geochemical reactions (as dissolved CO₂, bicarbonate or carbonate minerals),
- the chemical behaviour of caprock and its susceptibility to damage by the injected CO₂,
- the effect of the chemical changes on the porosity and permeability of the reservoir, which constrain fluid flow within the reservoir,
- the ability of geochemical codes and coupled reaction/transport codes to reproduce experimental observations and make accurate predictions.

The methodologies used within the SACS project lie on laboratory experiments (Task 3.2) and numerical modelling for the interpretation of these experiments (Task 3.3) and for the assessment of the geochemical state of the Utsira formation prior to CO₂ injection (Task 3.1).

The geochemical partners involved are two experimental groups (BGS and GEUS) and two modelling groups (BRGM and IFP). BRGM has been the co-ordinator of the geochemical work area since the beginning of the project. Regular discussions took place between the four partners, through e-mails, informal geochemical meetings just before or after steering committee meetings, and a geochemical meeting on March 30 in Copenhagen.

Preliminary work consisted in requesting and searching for geochemical data and rock samples relative to the Utsira formation and caprock, which were necessary to start the geochemical programme. Unfortunately, it turned out that only the following data and samples were available:

* *Samples of Utsira rock*: two frozen cores from the Sleipner field, coming from well 15/9-A-23 and corresponding to depths 1084.1-1085.0m (GEUS sample) and 1085.1-1086.0m (BGS sample). Dimensions about 1m long and 4 inches diameter.

* *Samples of Utsira caprock*: there exists no core from the Sleipner field or other fields, only cuttings.

* *Fluid data for the Utsira formation*: One detailed fluid chemical analysis is available in the Oseberg area (see p. 19 of the SACS Phase Zero report). Two other chemical analyses were carried out on the porewaters of the two core samples from the Sleipner field; however there were highly contaminated by drilling mud. The massive contamination and the lack of information about the composition of this mud (probably KCl + SO₄ + organic polymers...) prevented from doing any reliable assessment of the baseline fluid geochemistry at Sleipner. More details are given below in the Task 1.5 report, as the evaluation of formation fluids was the objective of this task.

* *Fluid data for the caprock formation*: no data will be available on the Sleipner field as only cuttings exist.

TASK 1.5. EVALUATION OF FORMATION FLUIDS (GEUS)

The objective of this task has been to collect available information on the formation water composition of the Utsira Formation and to carry out supplementary formation water analyses.

GEUS role has been to analyze fluid samples or extract pore water from preserved core if available.

Sampling

No fluid samples were available from the Utsira Formation. However, GEUS received 5 pieces of frozen 4" diameter core, in total 0.9 meter core covering the interval 1084.1 – 1085.0 meter MD from the 15/9-A23 well. The core pieces were preserved in ordinary plastic bags but appeared in a good condition. Immediately 4 plug samples (\varnothing ~38 mm) were drilled using dry nitrogen gas as a coolant, table 3.1.

Centrifuge extraction

The core plugs were trimmed to a length of 50 mm and, while still in a frozen condition, installed in specially designed centrifuge cups with integrated core holder and collection tube. After warming up to room temperature the 4 plugs were centrifuged at 3000 rpm for 20 minutes. A sufficient amount of pore water was extracted for analysis as shown in table 3.1.

Table 3.1 Frozen plugs drilled from preserved core (1084.1-1085.0 meter MD) in the well 15/9-A23, and used for formation water analysis.

Plug No.	Depth meter	Porosity %	Pore water extracted g
A-23.1	1084.13	42.5	16.4
A-23.2	1084.28	41.9	15.4
A-23.3	1084.65	40.71	16.1
A-23.4	1084.94	40.47	16.2

From inspection of material left from the 4 plugs drilled for formation water analysis, the Utsira sand from this core section appear as a gray unconsolidated, fine to medium grained, poorly sorted sand. The plugs used for formation water extraction were later used for mineralogical analysis.

Analytical data

The extracted water samples was analyzed by ion chromatography. Results are shown in table 3.2, together with analyses carried out by BGS on their core sample and the analysis from the Oseberg fluid.

As seen from the very high potassium concentration the core material was heavily contaminated by drilling mud. Water analyses from the nearby Oseberg Field typically have potassium concentrations ~200 ppm. An attempt to correct the analyses would require data on the chemical composition of the drilling mud, and even then it is questionable if a precise correction could be obtained considering the massive contamination.

It has not been possible to obtain any information on the mud composition. Therefore the best estimate of the Utsira Formation water composition is the analysis from the Oseberg field given in the SACS Phase 0 report (see table 3.2).

Table 3.2 Surface analysis of uncontaminated pore water samples from the Utsira Formation in the Oseberg field compared to analyses of pore water from the Utsira Formation in the Sleipner field cores (contaminated by drilling mud).

OSEBERG		SLEIPNER Analysed by GEUS				SLEIPNER Analysed by BGS	
Depth origin (m)		1084.13	1084.28	1084.65	1084.94	1085.1	1085.9
GWR (Sm³/Sm³)	0.14						
Gas composition							
CH4 (mol%)	96.64						
CO2 (mol%)	3.14						
pH	7.1					7.97	7.99
Salinity (g/l)	33-43						
Conc. (mg/l)							
Li						1.25	1.09
Na	10392	8200	7500	7700	8800	9138	8307
K	208	36400	36200	50400	38000	24081	29578
Mg	630	390	390	370	480	400	345
Ca	426	270	250	260	310	237	215
Sr	10					4.76	4.33
Ba	0.5					1.66	1.33
Mn						0.041	0.092
Fe	2					<0.01	<0.01
Al						<0.02	<0.02
Si						5.46	5.51
P						0.11	0.14
HCO3	707					262	311
TOC						5188	6796
TIC						31.6	37.2
Cl	18482	43100	41200	46600	41700	47612	49317
Br		443	423	521	406	415	442
NO3						7.65	5.73
SO4	n.d.	182	153	177	146	113	144

TASK 3.1. INITIAL FLUID/ROCK EQUILIBRIUM STATE OF THE UTSIRA FORMATION (BRGM)

The objective of this task is to describe the initial thermodynamic equilibrium state within the Utsira formation before CO₂ injection started. This baseline information will allow changes to the initial chemical conditions resulting from the CO₂ injection to be recognised and monitored.

Data available

The only data presently available and considered for this task are:

- a surface water analysis from the Oseberg field, 200 km north from the Sleipner field (see table 3.2),
- the mineralogical description of 2m core in the Sleipner field (well 15/9-A-23, 1084 to 1086 depth), as well as cuttings mineralogical description (see task 1.1 report).

The scarcity of the data and the fact that the water analysis and mineralogical description do not refer to the same location prevent from being able to do a precise and reliable assessment of the baseline geochemistry. The Oseberg analysis may not be fully representative of the Sleipner area, for instance regarding gas content, and do not report Al and Si contents which are crucial in studying aluminosilicate reactions. However, as the aqueous Na concentrations of the extracted porewaters (8-9 g/l), which were not affected by drilling mud contamination, are close to that of the Oseberg fluid (10 g/l, see Table 3.1), the decision of using the Oseberg analysis as

representative of the Utsira formation is presently an acceptable compromise. Direct measurements of Utsira fluid salinity are in agreement with this choice (33-43 g/l in the Oseberg field and 35-40 g/l in the Sleipner field, see SACS Task Zero report).

Comments on the chemical analysis of the Oseberg fluid

The fluid (table 3.2) is a Na-Cl brine with a TDS around 31 g/l, i.e., slightly lower than that of sea water (around 35 g/l). The chemical composition of this fluid probably results from a slight dilution of seawater by freshwater, followed by fluid-rock interaction processes. The aqueous Na and Cl concentrations indicate a similar dilution factor with respect to the concentrations of these elements in seawater and the Na/Cl ratio is close to that of seawater (Table 3.3). The K/Cl, Mg/Cl, SO₄/Cl ratios show a depletion in K, Mg, SO₄ with respect to a dilute seawater (Nordstrom et al., 1979) whereas the Ca/Cl, HCO₃/Cl and Sr/Cl ratios indicate an enrichment in Ca, HCO₃ and Sr (Table 3.3). These species, especially SO₄ and HCO₃, were affected by fluid-rock interactions.

Table 3.3 Comparison of the chemical composition of the Oseberg Utsira brine (Table 3.2) with seawater (Nordstrom et al., 1979). Concentrations are given in mg/l.

Species	Utsira brine	Seawater	Utsira brine / seawater
pH	7.1	8.2	0.87
Na	10 392	10 764	0.96
K	208	407	0.51
Ca	426	421	1.01
Mg	630	1 322	0.48
Cl	18 482	19 818	0.93
HCO ₃	707	123	5.75
SO ₄	low	2 776	low
Sr	10	8.3	1.20
Na/Cl	0.56	0.55	1.02
K/Cl	0.011	0.021	0.52
Ca/Cl	0.023	0.021	1.10
Mg/Cl	0.034	0.067	0.51
HCO ₃ /Cl	0.038	0.006	6.33
SO ₄ /Cl	low	0.140	low

Assessment of in situ fluid composition in the Oseberg field (23 °C, 7-8 MPa)

This was done from the available surface analysis. pH measurement was done at surface pressure and temperature (assumed to be 23°C), and therefore was affected by CO₂ degassing between down-hole and surface.

Several assumptions had to be made for the assessment of in situ fluid composition:

- Measured alkalinity was considered to represent bicarbonate alkalinity, as suggested in table 3.2. However it could also include a number of other species such as organic acids, but Oseberg formation water was not analysed for organic acids. Note that alkalinity is not affected by CO₂ degassing.
- As Al and Si concentrations were not measured, these parameters had to be calculated. They were determined assuming equilibrium with kaolinite and quartz (or chalcedony), respectively. Kaolinite is often associated to the control of aqueous aluminium concentrations, as at low temperature, kaolinite is considered as one of the most reactive alumino-silicate minerals, and as kaolinite is one of the only clay minerals for which thermodynamic parameters are relatively well defined. Quartz was considered as it is the dominant mineral of the Utsira formation. However calculations were also carried out considering chalcedony (a metastable silica phase) instead of quartz. This is because according to Kharaka et al. (1995) and Egeberg and Aagard (1989), aqueous silica in sedimentary basins is in equilibrium with quartz at temperature > 70°C but is generally considered to be in equilibrium with chalcedony at lower temperatures.
- In situ pH and total carbon concentration were calculated by two ways. Approach 1 uses the measured GWR, CO₂ molar percentage, pH and alkalinity. Approach 2 uses only the measured alkalinity and consider equilibrium with calcite in the reservoir. Approach 2 is probably more realistic to represent the chemical composition of the Utsira brine because (i) surface measurements could be not precise enough, (ii) calcite

was observed in the cores, (iii) the kinetics of carbonate minerals are fast, (iiii) saturation index calculations with respect to other carbonate minerals (disordered dolomite and strontianite) will confirm this assumption.

Aqueous speciation and saturation index calculations were done using the EQ3/6 software package, a reference code for geochemical modelling of water-rock interactions (Wolery, 1995). Its associated data0.com.R2 database was used. Most of this database has been generated from the SUPCRT92 database (Johnson et al., 1992), a reference software package for calculating the standard molal thermodynamic properties of minerals, gases, aqueous species and reactions. Other thermodynamic data (relative to montmorillonites for example) were added by Lawrence Livermore National Laboratory (LLNL) teams. The slight effect of pressure on the thermodynamic equilibrium constants is not considered. The extensive Debye-Hückel formalism (B-dot equation) was used to calculate the ion activity coefficients for electrically charged species. In the case of polar neutral aqueous species, the activity coefficients were set to unity. The activity of aqueous CO₂ was calculated from the expression after Drummond (1981). Iron and redox reactions (concerning pyrite, siderite) were not considered in saturation index calculations because of lack of information.

Calculation results are given in Table 3.4 and 3.5.

Assessment of in situ fluid composition in the Sleipner field (37 °C, 8-11 MPa)

This was achieved by heating the in situ Oseberg fluid composition from 23°C to 37°C, considering approach 2 as the most realistic approach.

Calculations were done using the EQ3/6 code as above. Another simulation was carried out using SCALESIM, a geochemical code built at BRGM (Azaroual et al., 1999), which takes into account the effect of pressure (assumed to be 10 Mpa) on thermodynamic constants and uses the Pitzer formalism for the calculation of activity coefficients (AI is not considered in SCALESIM).

Calculation results are given in Table 3.4 and 3.5.

Comments on the results of the calculations

The pH and CO₂ fugacity obtained by the approaches 1 and 2 are in the same order of magnitude (Tables 3.4 and 3.5). The CO₂ fugacity value found in approach 2 (0.035 bar at 23°C, 0.07 and 0.12 bar at 37°C depending on the modelling approach used) could be compared to that given by the relationship for CO₂ pressures versus temperature in hydrocarbon North Sea reservoirs of the norwegian continental shelf (Smith and Ehrenberg, 1989). This relationship, established for the temperature range 50-160°C, gives when extended to 23°C and 37°C CO₂ partial pressure of 0.097 and 0.18 bar respectively. Note that the calculations carried out with the SCALESIM code lead to higher pH, pCO₂ and total dissolved carbon. Further reflexions will be pursued within SAC II in order to relate CO₂ calculated fugacities with partial pressures and test the relationship of Smith and Ehrenberg over its range of application.

Saturation indices with respect to carbonate minerals (calcite, aragonite, disordered dolomite and strontianite) show that, whatever the approach, the fluid is close to equilibrium with respect to these minerals. Calcite and aragonite were actually observed in the rock samples (see Task 1.1). Disordered dolomite and strontianite were not mineralogically detected.

Saturation indices with respect to aluminosilicate minerals are dependent on the assumption on silica constraint. When dissolved silica is controlled by chalcedony, saturation indices calculated at 23°C and 37°C for approach 2 indicate that the Utsira brine is close to equilibrium with respect to illite, montmorillonites and K-feldspar, over-saturated with respect to muscovite and under-saturated with respect to anorthite, albite, paragonite, phlogopite, and pyrophyllite. When compared to the mineralogical analyses, K-feldspar, muscovite, illite, smectites (which can be represented by montmorillonites in modelling), considered as stable, were effectively observed. However, albite was also detected and appear to be thermodynamically unstable (slight under-saturation).

Approach 2 calculations using quartz instead of chalcedony differ mainly by the fact that illite and montmorillonites are unstable (slight under-saturation).

As discussed previously and confirmed here on the examination of CO₂ fugacities and saturation indices of carbonate and aluminosilicate minerals, Approach 2 is presently considered more realistic than Approach 1 to assess the baseline geochemistry of the Utsira formation.

However further calculations will be carried out within SACS II and refinements will be achieved working on thermodynamic data, mineralogical observations and results of the blank batch experiments. The latter will be of great interest for studying the baseline geochemistry before CO₂ injection.

Table 3.4 Assessment of in situ formation water composition at Oseberg and Sleipner from EQ3/6 and SCALESIM simulations – Si constrained by equilibrium with Chalcedony.

		OSEBERG			SLEIPNER	
		Surface measurement	Assessment of In situ conditions			
			Approach 1	Approach 2	Approach 2	Approach 2
			from measured pH, alkalinity, GWR and gas composition	from measured alkalinity and assumption of calcite equilibrium	Heating fluid from Oseberg approach 2 from 23 to 37°C, while maintaining equilibrium with calcite, kaolinite and chalcedony	Same approach as previously except for kaolinite - Effect of pressure (P=100 bar) is considered and Pitzer formalism is used
Température (°C)		23	23	23	37	37
GWR (Sm3/Sm3)		0.14				
CO2 (% mol)		3.14				
pH		7.1	7.03	6.73	6.57	6.53
Na (mg/l)		10392				
K (mg/l)		208				
Ca (mg/l)		426				
Mg (mg/l)		630				
Sr (mg/l)		10				
Ba (mg/l)		0.5				
HCO3 (mg/l) (Alkalinity)		707				
Cl (mg/l)		18482				
Al (mg/l)		not measured	Al constrained by equilibrium with Kaolinite			
Si (mg/l)		not measured	Si constrained by equilibrium with Chalcedony			
SO4 (mg/l)		not detected, assumed 1 mg/l				
fCO2			0.035	0.070	0.12	0.17
Total carbon (mole/kg h2o)			1.278E-02	1.390E-02	1.345E-02	1.504E-02
Total carbon (mg/kg sol HCO3)			757	823	796	
Si (mg/kg sol)			4.7	4.7	8.3	7.5
Al (mg/kg sol)			7.3E-05	4.6E-05	1.1E-04	n.d.
Salinity (g/kg h2o)			31.3	31.3	31.3	31,3
Saturation Index (log Q/K)						
Albite	NaAlSi3O8		-0.375	-0.671	-0.529	n.d.
Anorthite	CaAl2(SiO4)2		-8.504	-9.096	-8.243	n.d.
Aragonite	CaCO3		0.150	-0.144	-0.144	-0.140
Beidellite-Ca	Ca.165Al2.33Si3.67O10(OH)2		-0.791	-0.889	-0.723	n.d.
Beidellite-H	H.33Al2.33Si3.67O10(OH)2		-1.711	-1.711	-1.548	n.d.
Beidellite-K	K.33Al2.33Si3.67O10(OH)2		-0.883	-0.980	-0.904	n.d.
Beidellite-Mg	Mg.165Al2.33Si3.67O10(OH)2		-0.682	-0.780	-0.586	n.d.
Beidellite-Na	Na.33Al2.33Si3.67O10(OH)2		-0.586	-0.684	-0.568	n.d.
Calcite	CaCO3		0.295	0.000	0.000	0,000
Chalcedony	SiO2		0.000	0.000	0.000	0,000
Dolomite-dis	CaMg(CO3)2		0.658	0.069	0.255	n.d.
Illite	K0.6Mg0.25Al1.8Al0.5Si3.5O10(OH)2		-0.006	-0.333	-0.235	n.d.
K-Feldspar	KAlSi3O8		0.757	0.461	0.379	n.d.
Kaolinite	Al2Si2O5(OH)4		0.000	0.000	0.000	n.d.
Montmor-Ca	Ca.165Mg.33Al1.67Si4O10(OH)2		0.261	-0.032	0.173	n.d.
Montmor-K	K.33Mg.33Al1.67Si4O10(OH)2		0.240	-0.053	0.060	n.d.
Montmor-Mg	Mg.495Al1.67Si4O10(OH)2		0.441	0.147	0.375	n.d.
Montmor-Na	Na.33Mg.33Al1.67Si4O10(OH)2		0.533	0.239	0.392	n.d.
Muscovite	KAl3Si3O10(OH)2		1.164	0.868	0.826	n.d.
Paragonite	NaAl3Si3O10(OH)2		-0.869	-1.166	-0.952	n.d.
Phlogopite	KAlMg3Si3O10(OH)2		-1.657	-3.732	-2.534	n.d.
Pyrophyllite	Al2Si4O10(OH)2		-1.094	-1.094	-0.987	n.d.
Quartz	SiO2		0.273	0.273	0.261	0,261
Saponite-Ca	Ca.165Mg3Al.33Si3.67O10(OH)2		-0.431	-2.307	-1.074	n.d.
Saponite-H	H.33Mg3Al.33Si3.67O10(OH)2		-1.351	-3.129	-1.899	n.d.
Saponite-K	K.33Mg3Al.33Si3.67O10(OH)2		-0.522	-2.399	-1.255	n.d.
Saponite-Mg	Mg3.165Al.33Si3.67O10(OH)2		-0.321	-2.198	-0.939	n.d.
Saponite-Na	Na.33Mg3Al.33Si3.67O10(OH)2		-0.226	-2.103	-0.919	n.d.
Strontianite	SrCO3		0.441	0.147	0.013	-0,003
Talc	Mg3Si4O10(OH)2		-0.735	-2.514	-1.332	n.d.

Table 3.5 Assessment of in situ formation water composition at Oseberg and Sleipner from EQ3/6 simulations – Si constrained by equilibrium with Quartz.

		OSEBERG			SLEIPNER
		Surface measurement	Assessment of In situ conditions		
			Approach 1	Approach 2	Approach 2
			from measured pH, alkalinity, GWR and gas composition	from measured alkalinity and assumption of calcite equilibrium	Heating fluid from Oseberg approach 2 from 23 to 37°C, while maintaining equilibrium with calcite, kaolinite and quartz
Température (°C)		23	23	23	37
GWR (Sm3/Sm3)		0.14			
CO2 (% mol)		3.14			
pH		7.1	7.03	6.73	6.57
Na (mg/l)		10392			
K (mg/l)		208			
Ca (mg/l)		426			
Mg (mg/l)		630			
Sr (mg/l)		10			
Ba (mg/l)		0.5			
HCO3 (mg/l) (Alkalinity)		707			
Cl (mg/l)		18482			
Al (mg/l)		not measured	Al constrained by equilibrium with Kaolinite		
Si (mg/l)		not measured	Si constrained by equilibrium with Quartz		
SO4 (mg/l)		not detected, assumed 1 mg/l			
fCO2			0.035	0.070	0.12
Total carbon (mole/kg h2o)			1.278E-02	1.390E-02	1.345E-02
Total carbon (mg/kg sol HCO3)			757	823	796
Si (mg/kg sol)			2.5	2.5	4.5
Al (mg/kg sol)			1.4E-04	8.6E-05	2.0E-04
Salinity (g/kg h2o)			31.3	31.3	31.3
Saturation Index (log Q/K)					
Albite	NaAlSi3O8		-0.921	-1.217	-1.050
Anorthite	CaAl2(SiO4)2		-8.504	-9.096	-8.243
Aragonite	CaCO3		0.150	-0.144	-0.144
Beidellite-Ca	Ca.165Al2.33Si3.67O10(OH)2		-1.157	-1.254	-1.072
Beidellite-H	H.33Al2.33Si3.67O10(OH)2		-2.076	-2.076	-1.898
Beidellite-K	K.33Al2.33Si3.67O10(OH)2		-1.248	-1.346	-1.253
Beidellite-Mg	Mg.165Al2.33Si3.67O10(OH)2		-1.048	-1.145	-0.935
Beidellite-Na	Na.33Al2.33Si3.67O10(OH)2		-0.952	-1.050	-0.917
Calcite	CaCO3		0.295	0.000	0.000
Chalcedony	SiO2		-0.273	-0.273	-0.261
Dolomite-dis	CaMg(CO3)2		0.658	0.069	0.255
Illite	K0.6Mg0.25Al1.8Al0.5Si3.5O10(OH)2		-0.334	-0.660	-0.548
K-Feldspar	KAlSi3O8		0.211	-0.085	-0.142
Kaolinite	Al2Si2O5(OH)4		0.000	0.000	0.000
Montmor-Ca	Ca.165Mg.33Al1.67Si4O10(OH)2		-0.375	-0.668	-0.434
Montmor-K	K.33Mg.33Al1.67Si4O10(OH)2		-0.396	-0.689	-0.547
Montmor-Mg	Mg.495Al1.67Si4O10(OH)2		-0.196	-0.489	-0.232
Montmor-Na	Na.33Mg.33Al1.67Si4O10(OH)2		-0.103	-0.397	-0.215
Muscovite	KAl3Si3O10(OH)2		1.164	0.868	0.826
Paragonite	NaAl3Si3O10(OH)2		-0.869	-1.165	-0.952
Phlogopite	KAlMg3Si3O10(OH)2		-2.204	-4.278	-3.055
Pyrophyllite	Al2Si4O10(OH)2		-1.640	-1.640	-0.859
Quartz	SiO2		0.000	0.000	0.000
Saponite-Ca	Ca.165Mg3Al.33Si3.67O10(OH)2		-1.343	-3.219	-1.944
Saponite-H	H.33Mg3Al.33Si3.67O10(OH)2		-2.263	-4.041	-2.770
Saponite-K	K.33Mg3Al.33Si3.67O10(OH)2		-1.435	-3.311	-2.125
Saponite-Mg	Mg3.165Al.33Si3.67O10(OH)2		-1.234	-3.110	-1.809
Saponite-Na	Na.33Mg3Al.33Si3.67O10(OH)2		-1.139	-3.015	-1.790
Strontianite	SrCO3		0.441	0.147	0.013
Talc	Mg3Si4O10(OH)2		-1.828	-3.606	-2.374

TASK 3.2. GEOCHEMICAL LABORATORY EXPERIMENTS (BGS and GEUS)

The objective of this task is to determine the potential for reaction of the reservoir rock (Utsira sand) and caprock with injected CO₂, identify the key geochemical reactions (direction, magnitude and rate) and provide test cases to improve the ability of geochemical modelling packages to make accurate predictions.

The four partners of the geochemical programme decided to use a 'synthetic Oseberg fluid' in the experiments, as representative of the Utsira formation fluid (compromise).

BGS EXPERIMENTS

Activities at the British Geological Survey (BGS) are focused on 5 areas:-

- i) Long term batch experiments under in-situ conditions (involving Utsira sand, synthetic Oseberg porewater and CO₂).
- ii) Long term batch experiments at a temperature above in-situ conditions (involving Utsira sand, synthetic Oseberg porewater and CO₂).
- iii) CO₂ solubility measurements under conditions relevant to (i) and (ii) above.
- iv) Long term, long pathlength flow experiments (involving Utsira sand, synthetic Oseberg porewater and CO₂).
- v) Development of in-situ pH measuring technique.

Of the areas described above, (i) is by far the most important, and is where most effort has concentrated. Each of these are taken in turn below.

Long term batch experiments under in-situ conditions

A series of these experiments were initiated in early August 1999, and by the end of the reporting period will have been running for approximately 5 months. The aim of these experiments is to investigate the reactions caused by adding CO₂ to Utsira sand and synthetic Oseberg porewater. The experiments are being done in pairs, with each pair set up identically to one another. The only difference is of the timescale of reaction, which varies from 1 month to 24 months. When the results of the experiments are plotted over increasing time it should be possible to get information on the rates and magnitude of the geochemical changes.

Each pair of experiments consists of one pressurised with CO₂ and an 'experimental blank' pressurised with nitrogen. The experiment pressurised with nitrogen is useful for finding out just how close the Oseberg porewater is to equilibrium with the Utsira sand. In other words, the data from these experiments will help to compensate for the lack of information on baseline geochemistry at Sleipner. The experiment pressurised with CO₂ will allow observation of changes over and above those occurring in the experiments pressurised with nitrogen.

The equipment is relatively simple, and consists of a steel pressure vessel enclosing a PTFE liner (see Figure 3.1). A fixed weight of Utsira sand, a fixed volume of synthetic Oseberg porewater, and a fixed pressure of CO₂ are added to the pressure vessel at the start of the experiment. A constant pressure of CO₂ is maintained throughout the experiment (10 MPa to represent reservoir conditions). The experiments are held within an oven at 37°C. The simple design of the experiments is important in that there is relatively little to go wrong or maintain over the long run times being used in this study.

At the end of the experiment sampling proceeds in 2 steps. The initial step removes a fluid sample. This is done via a 'dip tube' (see Figure 3.1) and is similar to that used in previous studies (Gunter *et al.*, 1997). CO₂ pressure is maintained throughout this sampling procedure to ensure that the solution does not degass. Two fluid samples are taken into pressurised samplers. The first is for normal depressurisation and loss of CO₂. The second is reacted with 4M NaOH solution at 10 MPa pressure to convert the dissolved CO₂ to CO₃²⁻. Using this method degassing on depressurisation is minimised, and total dissolved inorganic carbon (i.e. mainly CO₂) is determined by titration against a known strength of acid (see Czernichowski-Lauriol *et al.*, 1996).

Figure 3.1 Schematic diagram of the batch equipment used by BGS.

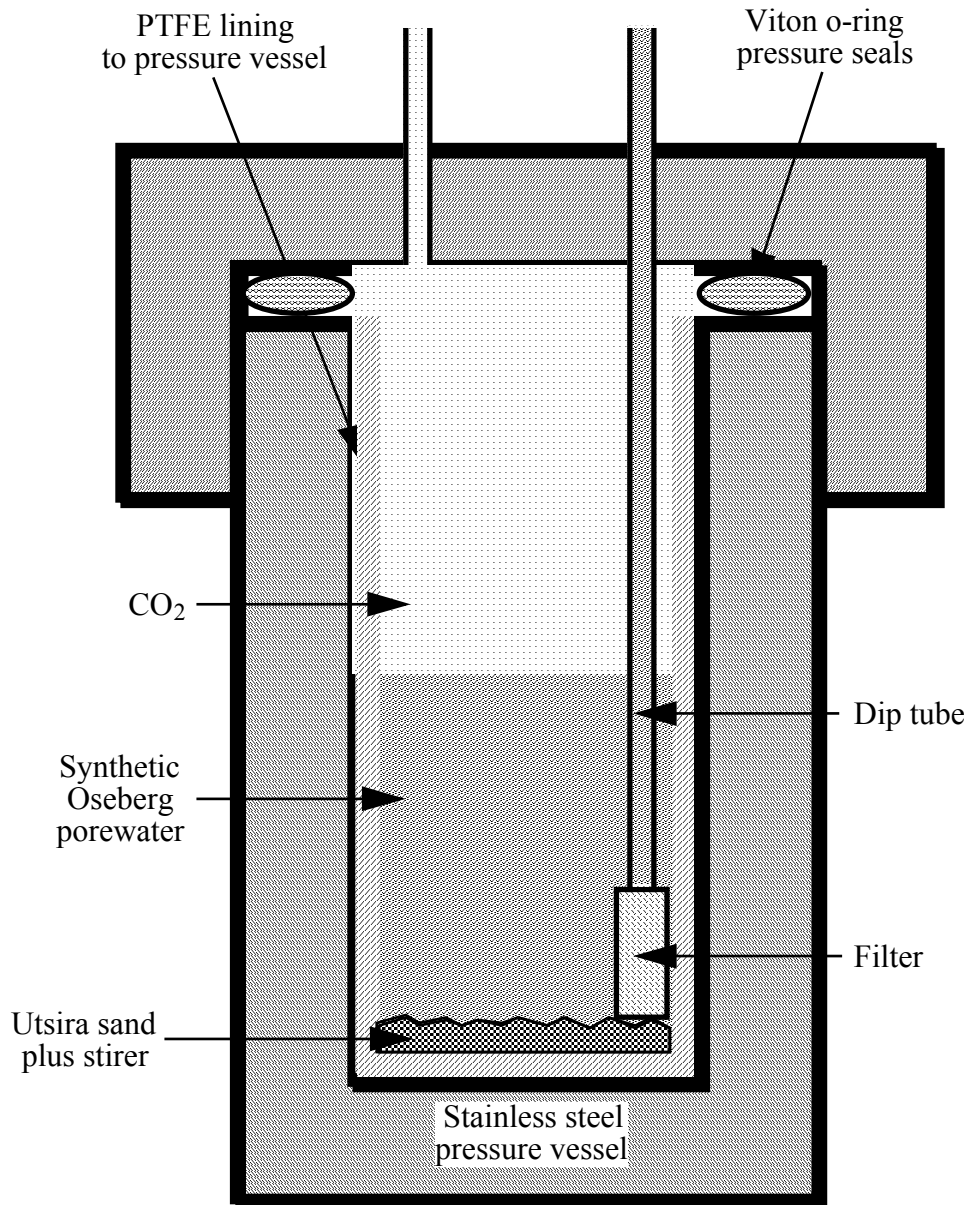


Table 3.6 Preliminary results from the BGS shorter-term experiments

INFORMATION FROM BGS BATCH EXPERIMENTS AT 37 °C									
		OSEBERG	SUP	1 MONTH REACTION		2 MONTHS REACTION		3 MONTHS REACTION	
		Oseberg composition from Task 0 report	Synthetic Utsira Porewater starting solution *	Run 859 CO ₂ expt 10 MPa CO ₂	Run 860 Blank 10 MPa N ₂	Run 838 CO ₂ expt 10 MPa CO ₂	Run 839 Blank 10 MPa N ₂	Run 840 CO ₂ expt 10 MPa CO ₂	Run 841 Blank 10 MPa N ₂
Exact duration				30 days	30 days	59 days	59 days	96 days	96 days
pH (7.1	7,77	6,62	7,82	6.68	8.03	6,43	7,82
Na	mg/l	10392	10306	9326	9400	10438	9979	10226	10528
K	mg/l	208	225	228	226	277	251	240	239
Mg	mg/l	630	633	580	578	659	622	625	629
Ca	mg/l	426	432	1577	332	1817	372	1840	376
Sr	mg/l	10	10,0	13,6	7,84	17,1	9,16	16,7	9,29
Ba	mg/l	0,5	0,31	2,12	4,22	2,78	3,80	2,44	3,70
Total Fe	mg/l	2	1,21	0,71	1,41	6,48	0,40	5,72	9,07
Al	mg/l	-	<2.00	<2.00	<2.00	7,44	3,04	<2.00	1,94
Total S	mg/l	-	1,05	23,3	11,2	33,2	15,3	34,1	16,9
Si	mg/l	-	BD	2,36	0,87	2,88	2,76	3,23	0,87
SiO ₂	mg/l	-	BD	5,06	1,86	6,16	5,90	6,91	1,86
Cl	mg/l	18482	18659	18166	17952	18849	18549	18556	18621
Br	mg/l	-	<2.00	<2.00	<6.00	<6,00	<6,00	<6,00	<6,00
SO ₄	mg/l	ND	<2.00	<2.00	<60.00	66,8	<60,0	68,2	<60,00
HCO ₃ **	mg/l	707	386	3102	300	1558	368	4423	349
Ionic balance	%	-	-	-2,27	-3,25	4,20	-1,77	-0,20	0,43
TIC (CO ₃ ²⁻) †	mol/l	-	-	0.58 ?	-	1,03	-	0.47 ?	-

* Average of 'E641A / SUP', 'E642 / SUP' and 'SUP for expts'

** Analyses done several days after sampling so be aware of possible decreases over time due to loss of CO₂ to the atmosphere. Alkalinity measurements by potentiometric titration.

†† CO₂-rich solutions captured in 4M NaOH whilst at 10 Mpa pressure. Potentiometric titrations represent total inorganic carbon (i.e. CO₂, H₂CO₃, HCO₃⁻, CO₃²⁻ etc).

? Analyses being checked/re-analysed as concentrations appear low.

Fluids analyses of the shorter-term experiments are presented in Table 3.6. Preliminary analysis of the data suggests that:

- The synthetic Oseberg porewater is probably fairly close to chemical equilibrium with the Utsira sand. However, the lack of Al and Si in the synthetic solution has induced probable dissolution of aluminosilicate phases.
- The presence of 10 MPa of CO₂ has initiated carbonate dissolution. This may be either calcite or aragonite (in shell fragments). This is probably a response to a decrease in pH on addition of CO₂.

The second sampling step involves removal of the solid reaction products. In order to reduce the possibility of precipitation of secondary phases on depressurisation, all remaining aqueous solution is displaced by high pressure dichloromethane (Gunter *et al.*, 1997). This is denser than the aqueous solution, which is removed from the top of the reactor. Once all the aqueous solution has been removed the vessel is slowly depressurised. The solids from the experiments are then dried in a warm temperature (<50°C) oven. Mineralogical analysis of the solid reaction products is ongoing.

Long term batch experiments at a temperature above in-situ conditions

These experiments have not started yet, though they are due to do so early in SACS II. They will be very similar to those described above, except for their higher temperature. Further details are given in Section 8 below.

CO₂ solubility measurements

The first few of these experiments have already started. They are aimed at providing data on exactly how much CO₂ can dissolve into the synthetic Oseberg formation water over a range of conditions. The conditions chosen vary between 8 - 12 MPa and 37 - 70 °C. These were chosen to cover actual in-situ conditions and conditions in all the experiments. Although CO₂ solubility can be predicted from literature data, it was felt important to have a SACS-specific database of information.

The experiments are very simple and use batch equipment similar to that described above. The only difference between these experiments and those above is the lack of Utsira sand, and their much shorter duration. Previous studies (Czernichowski-Lauriol *et al.*, 1996; Ellis & Golding, 1963; Stewart & Munjal, 1970) suggest that equilibrium can be obtained in just a few hours. As a consequence, each experiment is only run for a few days at most. It is likely that a matrix of 15 - 20 experiments will be conducted, arranged to cover a range of conditions of interest. No data are available at the moment as analysis has not started.

Long term, long pathlength flow experiments

These experiments have not started yet, though they are due to do so early in SACS II. They are aimed at providing the geochemical modelling groups with 'test cases' with which to 'benchmark' the various modelling packages being employed in SACS. Work undertaken on them during the reporting period has concentrated on devising a suitable experimental approach and obtaining the necessary equipment. In brief, two experiments are envisaged, both to run at 70 °C and 10 MPa, and have a duration of about 12 months. The elevated temperature was chosen so as to increase the possibility of achieving an observable reaction over a laboratory timescale whilst not encouraging the formation of unrepresentative secondary phases. This temperature also coincides with that of the batch experiments described above. Further details are given in Section 8 below.

pH measurement

After the start of the SACS project, discussions between BGS and BRGM highlighted the need for a method of directly measuring pH under the conditions of the experiments. This could then be used to independently check the modelled pH values. Unfortunately, 'off the shelf' pH electrodes are not available for pressures above about 1.5 MPa. Higher pressure versions do exist, but are large complex pieces of research equipment. However, an interesting possibility exists of transferring a technique developed to aid the understanding of uranium processing (Toews *et al.*, 1995). In essence, this uses spectroscopic techniques to monitor the change in colour of pH indicator solution. Comparison with pH buffer solutions then gives the actual pH of the solution.

In order for the above to be used in the current experimental programme, a high pressure optical cell was manufactured at BGS. This has now been pressure tested at 51 MPa, well in excess of the pressures in the SACS work. Calibration of this cell under atmospheric pressures is currently ongoing, and it is expected that by the end of the reporting period some calibration at pressure will have commenced. It is envisaged that use of this optical cell to determine in-situ pH in the experiments will become a standard technique in SACS II.

GEUS EXPERIMENTS

GEUS role has been to characterize the mineralogy of the sand, to supply standard core analysis data, to undertake dynamic flooding experiments at reservoir conditions and take fluid samples for chemical analysis. Delays have occurred due to lacking information on the Utsira Sand formation water composition and running in problems with new analytical instrumentation. CO₂ flooding experiments lagging behind will be carried out during SACS II.

Core material and sampling

GEUS received 5 pieces of frozen 4" diameter core, in total 0.9 meter core covering the interval 1084.1 – 1085.0 meter MD from the 15/9-A23 well. The core pieces were preserved in ordinary plastic bags but appeared in a good condition. Immediately 4 plug samples ($\varnothing \sim 38$ mm) were drilled using dry nitrogen gas as a coolant. These plugs were used for formation water analysis (Task 1.5) but also supplied routine core analysis data, Table 3.7. When frozen core was available it was obvious to take a number of frozen plugs for the dynamic flooding experiments. Finally the core was described and a number of small samples taken for petrographical characterization (Task 1.1).

From inspection of plug trims and material left from the 4 plugs drilled for formation water analysis, the Utsira sand from this core section appear as a gray unconsolidated, fine to medium grained, poorly sorted sand. The plugs used for formation water extraction were later used for mineralogical analysis. Three of the additional frozen plugs were installed in core holders to be used in the dynamic flooding experiments.

Core analysis data

The bulk volume of the frozen plugs are determined with a caliper before experiment. After extraction of pore water the loose sand is washed in methanol and dried at room temperature. The solid material (grain volume) is measured in a Helium porosimeter, and the pore volume calculated as the difference between the bulk and grain volume. The porosity and grain density data shown in table 3.1 thus represents the unconsolidated Utsira sand in an unconfined state.

Table 3.7 Standard core analysis data measured at room conditions for unconsolidated and unconfined Utsira sand in the depth interval 1084.1-1085.0 m in the well 15/9-A23.

Core analysis data:			
Plug No.	Depth	Porosity	Grain dens.
	meter	%	g/cc
A-23.1	1084.13	42.5	2.661
A-23.2	1084.28	41.9	2.657
A-23.3	1084.65	40.7	2.651
A-23.4	1084.94	40.5	2.658

The 3 frozen plugs taken for the dynamic flooding experiments cannot be analyzed for porosity and grain density before experiment, because this would require heating to room temperature, cleaning and measurement in a sample cup whereby the samples would fall apart. The determination of porosity will be carried out after completion of the flooding experiment. The core analysis data given in table 3.8 assumes the samples have a mean porosity as calculated from the plug samples in table 3.7. The liquid permeability was measured at a confining sleeve pressure of 10 bar during the cleaning procedure and after 10 pore volumes (PV's) of Synthetic Utsira Porewater (SUP) had been flushed through the core plugs. The first chemical data to check the cleaning state of the samples are shown in table 3.9. It appears that the core samples have been cleaned of drilling mud which had a high concentration of potassium.

Table 3.8 Standard core analysis data measured at room conditions for preserved Utsira sand plugs (taken as frozen plugs) from the depth interval 1084.1-1085.0 m in the well 15/9-A23. The porosity is assumed to be 41% based on the data in table 3.7.

Plug No.	Depth	Diameter	Length	Porosity *	BV	PV	Liq. Perm.	Flow rate
	meter	mm	mm	%	cc	cc	mD	ml/h
A-23.5	1084.46	38.33	75.46	41	87.07	35.70	760	499
A-23.6	1084.51	38.44	69.87	41	81.09	33.25	570	499
A-23.7	1084.71	38.65	76.64	41	89.92	36.87	990	499

* estimated value

Table 3.9 Chemical data measured regularly at GEUS during the dynamic flooding experiments. First data on porewater from 3 preserved plugs after flushing 10 PV's through the samples at room conditions. Results given in ppm.

ID	Na	K	Mg	Ca	Sr	Ba	Mn	Ti	Al	Fe	Si	Sampling date	Date of analysis
Nom. comp.	10392	208	630	426	10	1							
GEUS SUP	10250	268	580	172	9.7	0.47	0.013	0.251	0.26	1.08	0.39	11.10.99	17.11.99
A-23.5	10260	268	587	130	7.5	0.54	0.085	0.090	0.24	1.08	0.66	27.10.99	17.11.99
A-23.6	10350	227	713	171	6.4	0.38	0.046	0.100	0.32	1.26	0.70	28.10.99	17.11.99
A-23.7	10240	234	727	158	5.9	0.36	0.088	0.093	0.26	1.10	0.93	27.10.99	17.11.99
Method:	AAS		ICP-MS										

Nominal composition originates from an Oseberg Field water analysis

GEUS SUP is a sample of the synthetic Utsira porewater taken from a stock solution

The 3 core samples were then transferred to a reservoir condition rig, fig. 3.2, and the confining pressure slowly increased to a net overburden (NOB) of 100 bar (equal to 62 bar hydrostatic confinement used in the experiments). The porosity reduction was calculated from the amount of liquid produced during pressure increase from 10 to 100 bars NOB. The loading caused some rearrangement of the grains in the loose sand, and the high flowrates used during permeability measurement inevitably produced some fines out of the samples. We now have a stable permeability reading at a somewhat higher level than measured during the cleaning cycle, table 3.10.

Table 3.10 Overburden data (100 bar NOB) measured at room temperature for preserved Utsira sand plugs from the depth interval 1084.1-1085.0 m in the well 15/9-A23. The calculated porosity and volume data is based on the initial data in table 3.2. Sample 23.7 have corrected dimensions after a necessary change of sleeve.

Plug No.	Depth	Diameter	Length	BV	PV	Porosity	Liq. Perm.	Flow rate
	meter	mm	mm	@ 100 bar net overburden pressure				ml/h
A-23.5	1084.46	38.33	75.46	83.75	32.38	38.7	1170	700
A-23.6	1084.51	38.44	69.87	78.60	30.76	39.1	1450	700
A-23.7	1084.71	38.00	71.90	81.54	31.97	39.2	800	700

BV – sample bulk volume

PV – sample pore volume

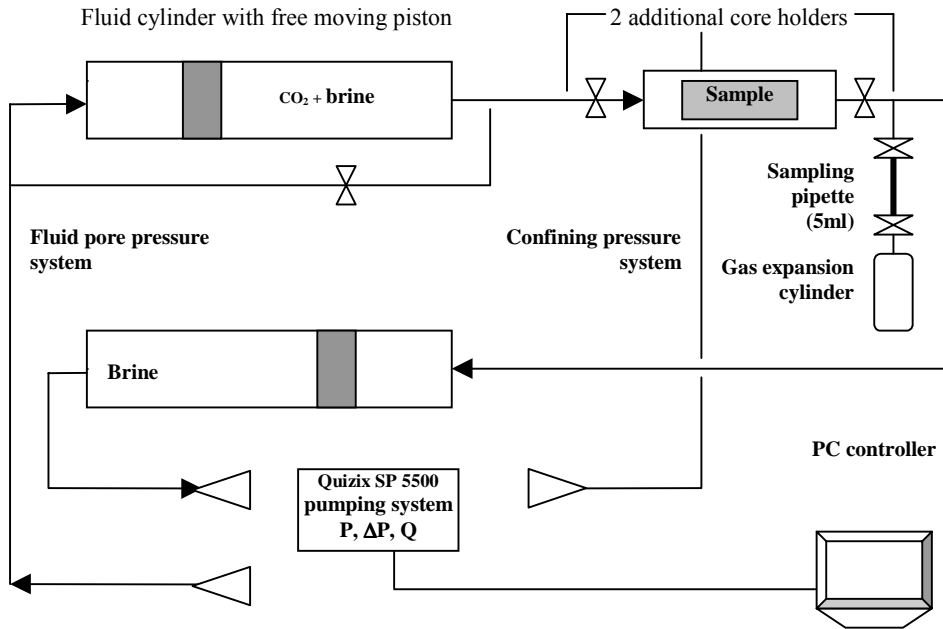
The next step will be to increase the temperature to 37 °C (reservoir temperature) and conduct a series of blind tests before the CO₂ saturated SUP is injected. A tracer study will be conducted after the preserved samples are completed. The experimental procedure applied in the reservoir condition rig is explained below in fig. 3.2.

The experimental conditions will be:

- Reservoir condition data
 - Depth, TVD_{ss} = 987 meter ~ 3238 feet
 - Gross overburden gradient = 0.9 psi/feet
 - Experiment overburden pressure = 2914 psi ~ 200 bar
 - Experiment pore pressure = 1457 psi ~ 100 bar
 - Experiment temperature = 37 °C
- Fluid/CO₂ data
 - Simulated formation brine saturated with CO₂ @ 100 bar
 - CO₂ density ~ 680 g/l @ 37 °C ~ 50 g CO₂/l brine

Fig. 3.2 GEUS reservoir condition rig for conducting CO₂ flooding experiments.

The pumping system delivers a flow of fresh CO₂–saturated brine for maximum reaction in the core samples, which are kept in an oven at constant temperature. The piston cylinders contain 800 or 1600 ml fluid and can be exchanged without losing the pore pressure in the system. Small fluid samples can be extracted under pore pressure with the pipette/gas expansion cylinder.



TASK 3.3. INTERPRET THE GEOCHEMICAL EXPERIMENTS (BRGM and IFP)

The objective of this task is to interpret the results of the laboratory experiments by numerical modelling, and test through the various experimental test cases the ability of geochemical codes and coupled reaction-transport codes to make accurate predictions.

Work achieved within the reported period consisted in code development and running tests under conditions close to the experimental conditions, to ensure accurate and robust calculations. Confrontation of modelling calculations and experimental results will only really begin within SACS II, as very few experimental results were available at the end of SACS.

BRGM MODELLING ACTIVITIES

Constraints on simulation conditions

Data from the Utsira core (well 15/9-A23, depth range 1079-1088 m)

As mentioned by Pearce et al. (1999), the Utsira formation is a sandy component of the Nordland Group of mainly Miocene age found in the Viking Graben area. It consists of a series of sand bodies, composed of fine grained, highly permeable sand with microfossil fragments in. In the Sleipner area, it has a thickness of 150 to 250 m. It has been suggested that the Utsira Formation sands were deposited in shallow marine conditions. However, they may represent stacked turbidite fan successions.

Several samples of the Utsira Formation were collected from the Sleipner area (Norwegian sector) by SINTEF Petroleum Research. Samples were mainly collected from one core (well 15/9-A23, depth range 1079-1088 m). The gamma and the resistivity log from the cored interval shows a rather uniform pattern and suggests a rather homogeneous sand unit. The samples were prepared, characterised and interpreted at SINTEF Petroleum Research. Samples from the core were distributed to the other SACS participants (1 m frozen core to GEUS and BGS).

Two segments from the core were available for SINTEF, one in depth range 1080-1081 m and one from 1087-1088 m. Detailed analyses were performed only on the first segment. The analyses involved microscopic observations of core and modal analyses (point counting). Four samples of frozen core (1084.13, 1084.28, 1084.65 and 1084.94 m) were petrographically and mineralogically characterised by GEUS using techniques such as microscopy, X-ray diffraction (XRD), scanning electron microscopy with element image analysis (SEM/EDX) and BET method (specific surface area determination by nitrogen absorption). A 1 m length of frozen core (1085 to 1086 m) was studied by BGS. The analyses involved mineralogical characterisation by XRD, petrographic analyses by SEM including backscattered scanning electron microscopy (BSEM) and limited electron probe microanalyses (EMPA) of selected minerals. Four subsamples were examined by a combination of these techniques to assess the mineralogical and petrographical variations of the Utsira at the sub-1 m scale.

The core segment ranging from 1080-1081 m (SINTEF) consists of grey sand which is very fine grained and well sorted. The sediment in the segment is homogeneous and no sedimentary structures can be observed macroscopically. The core segment examined by GEUS also consists of (unconsolidated) grey sand. The observations performed by BGS on the sandstone (1085 to 1086 m) show it is a medium grained, moderately to well sorted, very poorly cemented and friable subarkosic sand. Consequently, the core seems to be relatively homogeneous in a depth range from 1080 to 1086 m.

Common observations were performed on all the samples. The Utsira sand comprises predominant quartz with minor K-feldspar and traces of plagioclase (mainly albite), calcite, organic material (shell fragments, common bioclastic debris including foraminifera, radiolaria and sponge spicules), undifferentiated mica species (rare muscovite, biotite and glauconite) and chlorite. Rare heavy minerals include fine, subrounded ilmenite, zircon, garnet, apatite and rutile grains. Modal analyses performed by SINTEF yield porosities ranging from 27 to 31% while GEUS and BGS find porosity values ranging from 40.5 to 42.5%.

Detailed XRD analyses performed by BGS (Pearce et al., 1999) show that the clay mineralogy is generally uniform between 1085 and 1086 m. Several detrital grains are covered in a thin clay coating (< 10 µm) which is mainly constituted by smectite with minor illite and chlorite. Small quantities of kaolinite may also be present but could not be distinguished in the presence of chlorite. Chlorite in the samples is a relatively Fe-rich species. Illite

contains 0.7 K, 0.05 Fe per $(\text{Si, Al})_4\text{O}_{10}(\text{OH})_2$. In the $<2 \mu\text{m}$ fraction of all four samples, it was also found substantial quantities of cristobalite, quartz and aragonite.

In the BGS study, pyrite is a trace but commonly distributed authigenic mineral occurring as framboidal aggregates, especially within foraminifera tests. The most notable diagenetic modification is the development of two minor zeolites, phillipsite (dominant) and clinoptilolite. Although common, the zeolites form a very small component of the sand and do not represent a significant modification to porosity.

Selection of a rock composition representative of the Utsira Sand for geochemical modelling

Considering the results of the petrographical and mineralogical studies carried out by SINTEF, GEUS and BGS, it seems that the whole-rock mineralogy and the modal mineralogical composition given by BGS (from 1085 to 1086 m in well 15/9-A23) can be considered as representative of the Utsira Formation. For the purpose of geochemical modelling, the resulting composition has been simplified and slightly modified. The selected composition is reported in Table 3.11.

Table 3.11 Selected mineralogical composition of the Utsira Sand for geochemical modelling

Phase	Volume % (average)
Quartz	43.5
K-feldspar	6.0
Albite	1.5
Anorthite	0.3
Calcite	3.5
Muscovite	2.0
Chlorite	0.8
Smectite	0.3
Kaolinite	0.1
Porosity	42.0

Most of the trace phases (heavy metals, pyrite, zeolites) has been neglected for geochemical modelling. For thermodynamic reasons, calcium carbonate phases were assimilated to calcite, as aragonite observed by BGS is thermodynamically less stable than calcite and consequently, will either completely dissolve or be transformed into calcite in the experiments. Although not mineralogically detected, dis-dolomite will be considered in the modelling as saturation indices performed in Task 3.1 show equilibrium. Feldspars were divided into K-feldspars and plagioclases (mainly albite).

The presence of fine grains of cristobalite observed in the core samples by BGS could have a slight influence on the dissolved silica concentrations because this mineral, more soluble and less stable than quartz, could control these concentrations at low temperature. Chalcedony was not observed but is also considered to control the aqueous silica concentrations in sedimentary basins at low temperature (see Task 3.1). Then for geochemical modelling, chalcedony or cristobalite, which have the same chemical formula as quartz but not the same thermodynamic characteristics, could also be considered function of the experimental results.

In spite of the low observed amounts of kaolinite, this mineral was introduced in the modelling because it is often associated to the control of the aqueous aluminium concentrations (see Task 3.1).

In a first modelling approach, chlorite and smectites will be not considered because their amounts are low, their exact compositions are badly known, and the thermodynamic and kinetic data relative to these minerals are very inaccurate (Michard, 1983; Tardy and Duplay, 1992; Wolery, 1995; Aja, 1995). These minerals will be introduced in the geochemical modelling only if the experimental data suggest that they have a significant influence on the variations of mineralogical composition and fluid chemistry.

Finally, muscovite has been selected to represent the undifferentiated mica observed by all the SACS participants. However the thermodynamic data (inaccurate) for this mineral (Robie et al., 1978; Michard, 1983; Wolery, 1995) are generally in disagreement with the observations performed in oil field formations at low temperature (Sanjuan et al., 1995; 1999). Considering present thermodynamic data, muscovite is formed at the

expense of K-feldspar and kaolinite at low temperature, whereas its precipitation is only observed above 100°C in the oil field formations. In order to be in agreement with natural observations, Sanjuan and Girard (1999) proposed to arbitrarily use the chemical formula of the illite and the corresponding thermodynamic data from the EQ3/6 data0.com.R2 database (Wolery, 1995) to thermodynamically represent detrital muscovite at temperature lower than 100°C. At higher temperature, the observed diagenetic illite was represented by muscovite from the same database. In the SACS project, the chemical formula for muscovite and the corresponding data will be selected according to the obtained experimental results.

Modelling codes used by BRGM for the interpretation of the experiments

Batch experiments will be interpreted using geochemical codes, mainly EQ3/6 and SCALESIM (see Task 3.1), as well as a specific chemical simulator named 'UTSIRA simulator' developed by BRGM for the SACS project. Core flooded experiments will be interpreted using a coupled geochemical and transport code, specially developed for the SACS project by coupling the UTSIRA chemical simulator to the flow and transport code MARTHE. Details on code development are given below.

Construction of the geochemical UTSIRA simulator

The geochemical modelling strategy adopted in BRGM is based on the concept of Specific Chemical Simulator (SCS). For each new study a SCS is developed. The construction is facilitated thanks to the use of the modelling software ALLAN and NEPTUNIX, which automatically generate a FORTRAN code (Kervévan and Baranger, 1998).

The simulator solves the set of algebraic and/or ordinary differential equations that describes the geochemical system. As each SCS only includes relevant reaction mechanisms, the calculation-time is notably reduced compared to that of general chemical modelling software that take into account the wide range of chemical processes likely to occur in natural systems. This computational efficiency allows to perform reactive transport modelling using both the SCS and MARTHE, a 3D finite differences hydrogeological and transport code developed in BRGM (Thiéry, 1990).

The Utsira simulator was constructed under the ALLAN environment to calculate the evolutions with time of water solute speciation and water-rock-CO₂ interactions. It is designed (especially appropriate management of input/output data) to be further coupled to the Hydrogeological and Transport Code MARTHE.

As explained in the above chapter 'Constraints on simulation conditions', the Utsira simulator presently takes into account 9 minerals (calcite, quartz, dis-dolomite, albite, K-feldspar, kaolinite, muscovite, anorthite, illite), 32 aqueous reactions involving 42 relevant dissolved species (and 11 chemical elements: O, H, Na, K, Ca, Mg, Al, Si, S, C, Cl), and CO₂ as a gas phase. All reactions are listed in table 3.12.

The activity coefficients γ_i of charged species are calculated using the B-dot equation of Helgeson (1969). It is an extended Debye-Hückel model:

$$\log \gamma_i = -\frac{A_\gamma \cdot z_i^2 \cdot \sqrt{I}}{1 + \dot{a} \cdot B_\gamma \cdot \sqrt{I}} + \dot{B} \cdot I$$

with A_γ and B_γ the Debye-Hückel coefficients and \dot{B} the B-dot coefficient (all of them varying with temperature according to a polynomial function), z the charge and \dot{a} the hard core diameter of the specie, and I the ionic strength.

The activity coefficients of neutral polar species are set to unity.

The activity coefficient of (CO₂)_{aq} is computed according to the Drummond expression (1981):

$$\ln \gamma_i = (-1.0312 + 0.0012806 \cdot T + \frac{255.9}{T}) \cdot I - (0.4445 - 0.001606 \cdot T) \cdot (\frac{I}{1+I})$$

with temperature expressed in K.

Table 3.12 List of reactions included in the UTSIRA simulator

	Reactions	logKeq (37°C)
Calcite	$\text{CaCO}_3 + \text{H}^+ = \text{Ca}^{++} + \text{HCO}_3^-$	1,67
Quartz	$\text{SiO}_2 = \text{SiO}_2\text{aq}$	-3,78
Dis-Dolomite	$0.5 \text{CaMg}(\text{CO}_3)_2 + \text{H}^+ = 0,5 \text{Ca}^{++} + 0,5 \text{Mg}^{++} + \text{HCO}_3^-$	1,78
Albite	$\text{NaAlSi}_3\text{O}_8 = \text{Na}^+ + 3 \text{SiO}_2\text{aq} + \text{AlO}_2^-$	-19,26
K-Feldspar	$\text{KAlSi}_3\text{O}_8 = \text{K}^+ + 3 \text{SiO}_2\text{aq} + \text{AlO}_2^-$	-22,11
Kaolinite	$0.5 \text{Al}_2\text{Si}_2\text{O}_5(\text{OH}) = \text{SiO}_2\text{aq} + \text{AlO}_2^- + \text{H}^+ + 0,5 \text{H}_2\text{O}$	-18,77
Muscovite	$0.5 \text{KAl}_3\text{Si}_3\text{O}_{10}(\text{OH})_2 = 0,5 \text{K}^+ + 1,5 \text{SiO}_2\text{aq} + 1,5 \text{AlO}_2^- + \text{H}^+$	-26,53
Anorthite	$\text{CaAl}_2\text{Si}_2\text{O}_8 = \text{Ca}^{++} + 2 \text{SiO}_2\text{aq} + 2 \text{AlO}_2^-$	-18,81
Illite	$5/6 \text{K}_0,6\text{Mg}_0,25\text{Al}_2,3\text{Si}_3,5\text{O}_{10}(\text{OH})_2 = 0,5 \text{K}^+ + 1,25/6 \text{Mg}^{++} + 17,5/6 \text{SiO}_2\text{aq} + 11,5/6 \text{AlO}_2^- + \text{H}^+ + 2/6 \text{H}_2\text{O}$	-34,98
Gas	$(\text{CO}_2)_g + \text{H}_2\text{O} = \text{HCO}_3^- + \text{H}^+$	-7,89
	$\text{H}_2\text{O} = \text{OH}^- + \text{H}^+$	-13,62
	$\text{NaOH} + \text{H}^+ = \text{Na}^+ + \text{H}_2\text{O}$	14,43
	$\text{NaHSiO}_3 + \text{H}^+ = \text{Na}^+ + \text{SiO}_2 + \text{H}_2\text{O}$	8,22
	$\text{NaCl} = \text{Na}^+ + \text{Cl}^-$	0,74
	$\text{NaAlO}_2 = \text{Na}^+ + \text{AlO}_2^-$	0,67
	$\text{HSO}_4^- = \text{SO}_4^{--} + \text{H}^+$	-2,13
	$\text{CaCl}^+ = \text{Ca}^{++} + \text{Cl}^-$	0,67
	$\text{CaCl}_2 = \text{Ca}^{++} + 2 \text{Cl}^-$	0,67
	$(\text{CaCO}_3)\text{aq} + \text{H}^+ = \text{Ca}^{++} + \text{HCO}_3^-$	6,80
	$\text{CaHCO}_3^+ = \text{Ca}^{++} + \text{HCO}_3^-$	-1,07
	$\text{CaSO}_4 = \text{Ca}^{++} + \text{SO}_4^{--}$	-2,15
	$\text{KCl} = \text{K}^+ + \text{Cl}^-$	1,40
	$\text{KSO}_4 = \text{K}^+ + \text{SO}_4^{--}$	-0,91
	$\text{KHSO}_4 = \text{K}^+ + \text{SO}_4^{--} + \text{H}^+$	-1,03
	$\text{MgCl}^+ = \text{Mg}^{++} + \text{Cl}^-$	0,13
	$\text{MgCO}_3 + \text{H}^+ = \text{Mg}^{++} + \text{HCO}_3^-$	7,19
	$\text{MgHCO}_3^+ = \text{Mg}^{++} + \text{HCO}_3^-$	-1,06
	$(\text{CO}_2)\text{aq} + \text{H}_2\text{O} = \text{HCO}_3^- + \text{H}^+$	-6,29
	$\text{CO}_3^{--} + \text{H}^+ = \text{HCO}_3^-$	10,24
	$\text{HSiO}_3^- + \text{H}^+ = \text{SiO}_2(\text{aq}) + \text{H}_2\text{O}$	9,78
	$\text{Al}(\text{OH})^{++} + \text{H}_2\text{O} = \text{AlO}_2^- + 3 \text{H}^+$	-17,04
	$\text{Al}(\text{OH})_2^+ = \text{AlO}_2^- + 2 \text{H}^+$	-11,73
	$\text{Al}^{+++} + 2 \text{H}_2\text{O} = \text{AlO}_2^- + 4 \text{H}^+$	-21,66
	$\text{HAlO}_2 = \text{AlO}_2^- + \text{H}^+$	-6,21
	$(\text{NaHCO}_3)\text{aq} = \text{Na}^+ + \text{HCO}_3^-$	-0,06
	$\text{NaCO}_3^- + \text{H}^+ = \text{Na}^+ + \text{HCO}_3^-$	9,81
	$\text{NaSO}_4 = \text{Na}^+ + \text{SO}_4^{--}$	-0,82
	$\text{MgSO}_4 = \text{Mg}^{++} + \text{SO}_4^{--}$	-2,55
	$\text{HCl} = \text{H}^+ + \text{Cl}^-$	0,68
	$\text{CaOH}^+ = \text{Ca}^{++} + \text{OH}^-$	-1,15
	$\text{KOH} + \text{H}^+ = \text{K}^+ + \text{H}_2\text{O}$	14,46
	$\text{H}_2\text{SiO}_4^{--} + 2 \text{H}^+ = \text{SiO}_2\text{aq} + 2 \text{H}_2\text{O}$	22,96

Table 3.13 Mineral properties used for the kinetic model in the UTSIRA simulator

	log(k _{for})	Molar Volume (cm ³ /mol)	Mineral Diameter (cm)
Calcite	-9,19	36,934	0,05
Quartz	-17,08	22,688	0,02
Dis-Dolomite	-11,14	64,39	0,01
Albite	-16,12	100,25	0,02
K-Feldspar	-15,52	108,87	0,02
Kaolinite	-17,12	99,52	0,001
Muscovite	-17,22	140,71	0,01
Anorthite	-15,36	100,79	0,02
Illite	-16,3	138,94	0,01

The water activity is given by:

$$\log a_w = \frac{1}{55.51} \left(-\sum m + \frac{2}{3} A_\gamma \cdot I^{1.5} \cdot \sigma(\dot{a} \cdot B_\gamma \sqrt{I}) - \dot{B} \cdot I^2 \right)$$

with $\sum m$ the sum of molalities and $\sigma(x) = \frac{3}{x^3} \cdot \left(1 + x - \frac{1}{1+x} - 2 \cdot \ln(1+x) \right)$.

Dissolution-precipitation reaction of minerals are described according to the following kinetic law, derived from the Transition State Theory:

$$v_r = S \cdot k_{\text{for.}} \cdot (a_{\text{H}^+})^p \cdot (1 - Q/K) \quad \text{with} \quad S = s \cdot (6 V_m / d) \cdot n$$

with v_r the net reaction rate ($\text{mol} \cdot \text{s}^{-1} / \text{kg}_{\text{H}_2\text{O}}$), S the reactive surface ($\text{cm}^2 / \text{kg}_{\text{H}_2\text{O}}$), k_{for} the kinetic constant of the dissolution reaction ($\text{mol}/\text{cm}^2/\text{s}$), a_{H^+} the proton activity, Q the ionic activity product, K the total reaction equilibrium constant, s the reactive fraction of the mineral specific surface, V_m the mineral molar volume (cm^3/mol), d the mineral average diameter (cm) and n the mineral number of moles in the system (see table 3.13 for numerical values). Actually, the value of s is unknown, and in the simulator, this coefficient is often used as an adjustment parameter.

The simulator calls external FORTRAN subroutines that have been especially developed to calculate the thermodynamic and kinetic data according to the temperature.

$$\log(K_{\text{eq}}) = a + b \cdot T + c \cdot T^2 + d \cdot T^3$$

$$\log(k_{\text{for.}}) = \alpha \cdot T + \beta$$

All thermodynamic data (K_{eq} , coefficients a, b, c, d , A_γ , $B_\gamma \dots$) come from the data0.com.R2 database of the EQ3/6 v7.2b software package (Wolery, 1995).

The linear interpolation for the kinetic was obtained from data provided at 25°C and 60°C (Sanjuan and Girard, 1999).

A validation stage of the UTSIRA simulator is absolutely necessary before coupling the SCS with a hydrogeological code. For that purpose, code-to-code verifications were carried out with the EQ3/6 code. Simulations were performed to compare the results generated by EQ6 and UTSIRA simulator, respecting to aqueous speciation. Two types of water were tested:

- The first one represents the Utsira formation fluid at Sleipner prior to CO_2 injection, as assessed in Task 3.1, with the following assumptions: Si constrained by quartz, Al by kaolinite and in situ conditions assessed by approach 1 using measured surface parameters (hence no calcite equilibrium). This water does not appear in table 3.5 as only approach 2 was reported in the Sleipner column.
- The second type of water tested represents the Utsira formation fluid saturated with CO_2 at Sleipner. The composition of this fluid was obtained from the first type of water by adding carbon dioxide until reaching the CO_2 solubility value given by Enick and Klara (1990) and also reported in the previous CO_2 Joule report (Holloway et al., 1996). At Sleipner reservoir conditions, i.e. 37°C, 10 MPa and 3% salinity, the CO_2 solubility is about 47g per kg of brine, which corresponds to 1.1 moles of carbon per kilogram of solvent water (carbon molality).

Aqueous speciation, pH and CO_2 fugacity for these two waters are given in tables 3.14 and 3.15, with comparison between the results of Utsira simulator and EQ3/6 which shows very good agreement.

Table 3.14 Aqueous speciation, pH and CO₂ fugacity for a water representative of the Utsira formation fluid at Sleipner prior to CO₂ injection. Comparison of EQ3/6 and UTSIRA simulator results.

UTSIRA SIMULATOR RESULTS					EQ3/6 RESULTS																																																																			
Temperature : 37 °C					Temperature : 37 °C																																																																			
pH : 6.954					pH : 6.971																																																																			
Water activity : 0.98334					Water activity : 0.98334																																																																			
Total amount of water : 5.55084E+01 mol					Total amount of water : 5.55084E+01 mol																																																																			
Total mass of water : 1,00000E+00 kg					Total mass of water : 1,00000E+00 kg																																																																			
Ionic strength : 5,474317E-01 (molal scale)					Ionic strength : 5,474317E-01 (molal scale)																																																																			
Sum of molalities : 1,0162200 mol/kg					Sum of molalities : 1,0162199 mol/kg																																																																			
Species	Molality (mol/kg)	log molality	log gamma	log activity	Species	Molality (mol/kg)	log molality	log gamma	log activity																																																															
Clm	5,0690E-01	-0,2951	-0,1998	-0,4949	Cl-	5,0692E-01	-0,2951	-0,1831	-0,4782																																																															
Nap	4,3790E-01	-0,3586	-0,1723	-0,5309	Na+	4,3786E-01	-0,3587	-0,1890	-0,5477																																																															
Mgp2	2,2900E-02	-1,6402	-0,4995	-2,1400	Mg++	2,2898E-02	-1,6402	-0,5330	-2,1732																																																															
NaCl	1,7170E-02	-1,7652	0,0000	-1,7650	NaCl(aq)	1,7171E-02	-1,7652	0,0000	-1,7652																																																															
Cap2	1,0160E-02	-1,9931	-0,6031	-2,5960	Ca++	1,0159E-02	-1,9931	-0,6366	-2,6297																																																															
HCO3m	8,6460E-03	-2,0632	-0,1723	-2,2350	HCO3-	8,6464E-03	-2,0632	-0,1556	-2,2187																																																															
Kp	5,3350E-03	-2,2729	-0,1998	-2,4730	K+	5,3353E-03	-2,2728	-0,2165	-2,4894																																																															
MgClp	2,5630E-03	-2,5913	-0,1723	-2,7640	MgCl+	2,5627E-03	-2,5913	-0,1890	-2,7803																																																															
NaHCO3	1,9660E-03	-2,7064	0,0000	-2,7060	NaHCO3(aq)	1,9663E-03	-2,7064	0,0000	-2,7064																																																															
CO2	1,1330E-03	-2,9458	0,0537	-2,8920	CO2(aq)	1,1329E-03	-2,9458	0,0537	-2,8922																																																															
MgHCO3	7,1900E-04	-3,1433	-0,1723	-3,3160	MgHCO3+	7,1898E-04	-3,1433	-0,1890	-3,3323																																																															
CaClp	2,5520E-04	-3,5931	-0,1723	-3,7650	CaCl+	2,5525E-04	-3,5930	-0,1890	-3,7820																																																															
CaHCO3	2,5500E-04	-3,5935	-0,1723	-3,7660	CaHCO3+	2,5495E-04	-3,5935	-0,1890	-3,7825																																																															
SiO2	1,6510E-04	-3,7823	0,0000	-3,7820	SiO2(aq)	1,6513E-04	-3,7822	0,0000	-3,7822																																																															
CaCl2	5,5480E-05	-4,2559	0,0000	-4,2560	CaCl2(aq)	5,5478E-05	-4,2559	0,0000	-4,2559																																																															
KCl	4,3260E-05	-4,3639	0,0000	-4,3640	KCl(aq)	4,3256E-05	-4,3640	0,0000	-4,3640																																																															
MgCO3	2,4490E-05	-4,6110	0,0000	-4,6110	MgCO3(aq)	2,4488E-05	-4,6110	0,0000	-4,6110																																																															
CaCO3	2,1230E-05	-4,6731	0,0000	-4,6730	CaCO3(aq)	2,1230E-05	-4,6730	0,0000	-4,6730																																																															
CO3m2	1,4260E-05	-4,8459	-0,6720	-5,5180	CO3--	1,4265E-05	-4,8457	-0,6386	-5,4843																																																															
SO4m2	5,1910E-06	-5,2847	-0,7580	-6,0430	SO4--	5,1913E-06	-5,2847	-0,7245	-6,0093																																																															
NaCO3m	3,5730E-06	-5,4470	-0,1723	-5,6190	NaCO3-	3,5726E-06	-5,4470	-0,1556	-5,6026																																																															
NaSO4m	2,6220E-06	-5,5814	-0,1723	-5,7540	NaSO4-	2,6220E-06	-5,5814	-0,1556	-5,7369																																																															
NaHSiO	2,5720E-06	-5,5897	0,0000	-5,5900	NaHSiO3(aq)	2,5719E-06	-5,5897	0,0000	-5,5897																																																															
MgSO4	2,3480E-06	-5,6293	0,0000	-5,6290	MgSO4(aq)	2,3479E-06	-5,6293	0,0000	-5,6293																																																															
HSiO3m	3,6270E-07	-6,4405	-0,1723	-6,6130	HSiO3-	3,6261E-07	-6,4406	-0,1556	-6,5961																																																															
OHm	3,3470E-07	-6,4753	-0,1998	-6,6750	OH-	3,3463E-07	-6,4754	-0,1831	-6,6585																																																															
CaSO4	3,2680E-07	-6,4857	0,0000	-6,4860	CaSO4(aq)	3,2678E-07	-6,4857	0,0000	-6,4857																																																															
Hp	1,3910E-07	-6,8567	-0,0977	-6,9540	H+	1,3905E-07	-6,8568	-0,1144	-6,9712																																																															
KSO4m	3,6480E-08	-7,4379	-0,1723	-7,6100	KSO4-	3,6484E-08	-7,4379	-0,1556	-7,5934																																																															
AlO2m	1,3770E-08	-7,8611	-0,1723	-8,0330	AlO2-	1,3766E-08	-7,8612	-0,1556	-8,0167																																																															
NaOH	9,6860E-09	-8,0139	0,0000	-8,0140	NaOH(aq)	9,6869E-09	-8,0138	0,0000	-8,0138																																																															
HCl	7,4420E-09	-8,1283	0,0000	-8,1280	HCl(aq)	7,4422E-09	-8,1283	0,0000	-8,1283																																																															
CaOHp	4,7120E-09	-8,3268	-0,1723	-8,4990	CaOH+	4,7119E-09	-8,3268	-0,1890	-8,5158																																																															
HAIO2	1,6730E-09	-8,7765	0,0000	-8,7760	HAIO2(aq)	1,6732E-09	-8,7765	0,0000	-8,7765																																																															
NaAlO2	5,7660E-10	-9,2391	0,0000	-9,2390	NaAlO2(aq)	5,7659E-10	-9,2391	0,0000	-9,2391																																																															
KOH	1,0340E-10	-9,9855	0,0000	-9,9850	KOH(aq)	1,0340E-10	-9,9855	0,0000	-9,9855																																																															
AlOH2p	9,2100E-11	-10,0357	-0,1723	-10,2100	Al(OH)2+	9,2105E-11	-10,0357	-0,1890	-10,2247																																																															
HSO4m	2,0050E-11	-10,6979	-0,1723	-10,8700	HSO4-	2,0047E-11	-10,6979	-0,1556	-10,8535																																																															
AlOHp2	8,1410E-12	-11,0893	-0,7580	-11,8500	AlOH++	7,3309E-12	-11,1348	-0,7459	-11,8808																																																															
H2SiO4	8,1320E-13	-12,0898	-0,7580	-12,8500	H2SiO4--	8,1325E-13	-12,0898	-0,7245	-12,8143																																																															
Alp3	7,6400E-14	-13,1169	-1,0630	-14,1800	Al+++	7,6392E-14	-13,1170	-1,1130	-14,2300																																																															
KHSO4	3,6200E-15	-14,4413	0,0000	-14,4400	KHSO4(aq)	3,6197E-15	-14,4413	0,0000	-14,4413																																																															
<table border="1"> <thead> <tr> <th>Gas</th> <th>log(fugacity)</th> <th>fugacity</th> </tr> </thead> <tbody> <tr> <td>g0001</td> <td>-1,29E+00</td> <td>5,11E-02</td> </tr> </tbody> </table>					Gas	log(fugacity)	fugacity	g0001	-1,29E+00	5,11E-02	<table border="1"> <thead> <tr> <th>Gas</th> <th>Log</th> <th>Fugacity</th> </tr> </thead> <tbody> <tr> <td>CO2(g)</td> <td>-1,292</td> <td>5,10E-02</td> </tr> </tbody> </table>					Gas	Log	Fugacity	CO2(g)	-1,292	5,10E-02																																																			
Gas	log(fugacity)	fugacity																																																																						
g0001	-1,29E+00	5,11E-02																																																																						
Gas	Log	Fugacity																																																																						
CO2(g)	-1,292	5,10E-02																																																																						
<table border="1"> <thead> <tr> <th></th> <th>Input File :</th> <th>Output file at t=102,16146</th> </tr> </thead> <tbody> <tr><td>Ho</td><td>1,198671E-02</td><td>1,159002E-02</td></tr> <tr><td>Oo</td><td>3,779604E-02</td><td>3,759770E-02</td></tr> <tr><td>Alo</td><td>1,611574E-08</td><td>1,611574E-08</td></tr> <tr><td>Cao</td><td>1,074641E-02</td><td>1,074641E-02</td></tr> <tr><td>Clo</td><td>5,270593E-01</td><td>5,270593E-01</td></tr> <tr><td>Co</td><td>1,278300E-02</td><td>1,278300E-02</td></tr> <tr><td>Ko</td><td>5,378551E-03</td><td>5,378551E-03</td></tr> <tr><td>Mgo</td><td>2,620624E-02</td><td>2,620624E-02</td></tr> <tr><td>Nao</td><td>4,570086E-01</td><td>4,570086E-01</td></tr> <tr><td>So</td><td>1,052449E-05</td><td>1,052449E-05</td></tr> <tr><td>Sio</td><td>1,680689E-04</td><td>1,680689E-04</td></tr> <tr><td>H2Oo</td><td>5,550824E+01</td><td>5,550844E+01</td></tr> </tbody> </table>						Input File :	Output file at t=102,16146	Ho	1,198671E-02	1,159002E-02	Oo	3,779604E-02	3,759770E-02	Alo	1,611574E-08	1,611574E-08	Cao	1,074641E-02	1,074641E-02	Clo	5,270593E-01	5,270593E-01	Co	1,278300E-02	1,278300E-02	Ko	5,378551E-03	5,378551E-03	Mgo	2,620624E-02	2,620624E-02	Nao	4,570086E-01	4,570086E-01	So	1,052449E-05	1,052449E-05	Sio	1,680689E-04	1,680689E-04	H2Oo	5,550824E+01	5,550844E+01	<table border="1"> <thead> <tr> <th></th> <th>Elements Totals :</th> </tr> </thead> <tbody> <tr><td>Ho</td><td>1,110285E+02</td></tr> <tr><td>Oo</td><td>5,554604E+01</td></tr> <tr><td>Alo</td><td>1,611574E-08</td></tr> <tr><td>Cao</td><td>1,074641E-02</td></tr> <tr><td>Clo</td><td>5,270593E-01</td></tr> <tr><td>Co</td><td>1,278300E-02</td></tr> <tr><td>Ko</td><td>5,378551E-03</td></tr> <tr><td>Mgo</td><td>2,620624E-02</td></tr> <tr><td>Nao</td><td>4,570086E-01</td></tr> <tr><td>So</td><td>1,052449E-05</td></tr> <tr><td>Sio</td><td>1,680689E-04</td></tr> </tbody> </table>						Elements Totals :	Ho	1,110285E+02	Oo	5,554604E+01	Alo	1,611574E-08	Cao	1,074641E-02	Clo	5,270593E-01	Co	1,278300E-02	Ko	5,378551E-03	Mgo	2,620624E-02	Nao	4,570086E-01	So	1,052449E-05	Sio	1,680689E-04
	Input File :	Output file at t=102,16146																																																																						
Ho	1,198671E-02	1,159002E-02																																																																						
Oo	3,779604E-02	3,759770E-02																																																																						
Alo	1,611574E-08	1,611574E-08																																																																						
Cao	1,074641E-02	1,074641E-02																																																																						
Clo	5,270593E-01	5,270593E-01																																																																						
Co	1,278300E-02	1,278300E-02																																																																						
Ko	5,378551E-03	5,378551E-03																																																																						
Mgo	2,620624E-02	2,620624E-02																																																																						
Nao	4,570086E-01	4,570086E-01																																																																						
So	1,052449E-05	1,052449E-05																																																																						
Sio	1,680689E-04	1,680689E-04																																																																						
H2Oo	5,550824E+01	5,550844E+01																																																																						
	Elements Totals :																																																																							
Ho	1,110285E+02																																																																							
Oo	5,554604E+01																																																																							
Alo	1,611574E-08																																																																							
Cao	1,074641E-02																																																																							
Clo	5,270593E-01																																																																							
Co	1,278300E-02																																																																							
Ko	5,378551E-03																																																																							
Mgo	2,620624E-02																																																																							
Nao	4,570086E-01																																																																							
So	1,052449E-05																																																																							
Sio	1,680689E-04																																																																							

Table 3.15 Aqueous speciation, pH and CO₂ fugacity for a water representative of the Utsira formation fluid at Sleipner saturated with CO₂. Comparison of EQ3/6 and UTSIRA simulator results.

UTSIRA SIMULATOR RESULTS					EQ3/6 RESULTS				
Temperature : 37 °C					Temperature : 37 °C				
pH : 3.99					pH : 4.007				
Water activity : 0.96426					Water activity : 0.96426				
Total amount of water : 5.55082E+01 mol					Total amount of water : 5.55082E+01 mol				
Total mass of water : 9.99997E-01 kg					Total mass of water : 9.99997E-01 kg				
Ionic strength : 5.476005E-01 (molal scale)					Ionic strength : 5.476005E-01 (molal scale)				
Sum of molalities : 2.1039400 mol/kg					Sum of molalities : 2.1039405 mol/kg				
Species	Molality (mol/kg)	log molality	log gamma	log activity	Species	Molality (mol/kg)	log molality	log gamma	log activity
CO2	1,0890E+00	0,0370	0,0537	0,0905	CO2(aq)	1,0885E+00	0,0368	0,0537	0,0905
Clm	5,0690E-01	-0,2951	-0,1998	-0,4949	Cl-	5,0691E-01	-0,2951	-0,1831	-0,4782
Nap	4,3780E-01	-0,3587	-0,1723	-0,5310	Na+	4,3783E-01	-0,3587	-0,1890	-0,5477
Mgp2	2,2900E-02	-1,6402	-0,4996	-2,1400	Mg++	2,2905E-02	-1,6401	-0,5330	-2,1731
NaCl	1,7170E-02	-1,7652	0,0000	-1,7650	NaCl(aq)	1,7169E-02	-1,7653	0,0000	-1,7653
Cap2	1,0170E-02	-1,9927	-0,6032	-2,5960	Ca++	1,0174E-02	-1,9925	-0,6366	-2,6291
HCO3m	8,8440E-03	-2,0534	-0,1723	-2,2260	HCO3-	8,8440E-03	-2,0533	-0,1556	-2,2089
Kp	5,3350E-03	-2,2729	-0,1998	-2,4730	K+	5,3353E-03	-2,2728	-0,1890	-2,4894
MgClp	2,5630E-03	-2,5913	-0,1723	-2,7630	MgCl+	2,5634E-03	-2,5912	-0,1890	-2,7802
NaHCO3	2,0110E-03	-2,6966	0,0000	-2,6970	NaHCO3(aq)	2,0110E-03	-2,6966	0,0000	-2,6966
MgHCO3	7,3560E-04	-3,1334	-0,1723	-3,3060	MgHCO3+	7,3561E-04	-3,1334	-0,1890	-3,3224
CaHCO3	2,6110E-04	-3,5832	-0,1723	-3,7550	CaHCO3+	2,6114E-04	-3,5831	-0,1890	-3,7721
CaClp	2,5560E-04	-3,5924	-0,1723	-3,7650	CaCl+	2,5559E-04	-3,5925	-0,1890	-3,7815
SiO2	1,6810E-04	-3,7744	0,0000	-3,7750	SiO2(aq)	1,6807E-04	-3,7745	0,0000	-3,7745
Hp	1,2810E-04	-3,8925	-0,0977	-3,9900	H+	1,2810E-04	-3,8925	-0,1144	-4,0069
CaCl2	5,5550E-05	-4,2553	0,0000	-4,2550	CaCl2(aq)	5,5549E-05	-4,2553	0,0000	-4,2553
KCl	4,3250E-05	-4,3640	0,0000	-4,3640	KCl(aq)	4,3253E-05	-4,3640	0,0000	-4,3640
HCl	6,8560E-06	-5,1639	0,0000	-5,1640	HCl(aq)	6,8557E-06	-5,1639	0,0000	-5,1639
SO4m2	5,1820E-06	-5,2855	-0,0440	-5,3300	SO4--	5,1821E-06	-5,2855	-0,0726	-6,0101
NaSO4m	2,6170E-06	-5,5822	-0,1723	-5,7550	NaSO4-	2,6168E-06	-5,5822	-0,1556	-5,7378
MgSO4	2,3440E-06	-5,6300	0,0000	-5,6300	MgSO4(aq)	2,3441E-06	-5,6300	0,0000	-5,6300
CaSO4	3,2660E-07	-6,4860	0,0000	-6,4860	CaSO4(aq)	3,2661E-07	-6,4860	0,0000	-6,4860
KSO4m	3,6410E-08	-7,4388	-0,1723	-7,6110	KSO4-	3,6415E-08	-7,4387	-0,1556	-7,5943
MgCO3	2,7200E-08	-7,5654	0,0000	-7,5650	MgCO3(aq)	2,7196E-08	-7,5655	0,0000	-7,5655
CaCO3	2,3600E-08	-7,6271	0,0000	-7,6270	CaCO3(aq)	2,3604E-08	-7,6270	0,0000	-7,6270
HSO4m	1,8430E-08	-7,7345	-0,1723	-7,9070	HSO4-	1,8433E-08	-7,7344	-0,1556	-7,8900
CO3m2	1,5840E-08	-7,8002	-0,6721	-8,4720	CO3--	1,5840E-08	-7,8002	-0,6386	-8,4389
Alp3	1,4460E-08	-7,8398	-1,0630	-8,9030	Al+++	1,4602E-08	-7,8356	-1,1130	-8,9486
NaCO3m	3,9660E-09	-8,4016	-0,1723	-8,5740	NaCO3-	3,9664E-09	-8,4016	-0,1556	-8,5572
NaHSiO	2,7860E-09	-8,5550	0,0000	-8,5550	NaHSiO3(aq)	2,7860E-09	-8,5550	0,0000	-8,5550
AlOHp2	1,6400E-09	-8,7852	-0,7580	-9,5430	AlOH++	1,4916E-09	-8,8264	-0,7460	-9,5723
HSiO3m	3,9290E-10	-9,4057	-0,1723	-9,5780	HSiO3-	3,9284E-10	-9,4058	-0,1556	-9,5713
OHm	3,5620E-10	-9,4483	-0,1998	-9,6480	OH-	3,5620E-10	-9,4483	-0,1831	-9,6314
AlOH2p	1,9740E-11	-10,7047	-0,1723	-10,8800	Al(OH)2+	1,9946E-11	-10,7001	-0,1890	-10,8891
NaOH	1,0310E-11	-10,9867	0,0000	-10,9900	NaOH(aq)	1,0310E-11	-10,9867	0,0000	-10,9867
CaOHp	5,0220E-12	-11,2991	-0,1723	-11,4700	CaOH+	5,0225E-12	-11,2991	-0,1890	-11,4881
KHSO4	3,3280E-12	-11,4778	0,0000	-11,4800	KHSO4(aq)	3,3282E-12	-11,4778	0,0000	-11,4778
HAlO2	3,8940E-13	-12,4096	0,0000	-12,4100	AlSO4+	1,7389E-12	-11,7597	-0,1890	-11,9487
KOH	1,1010E-13	-12,9582	0,0000	-12,9600	HAlO2(aq)	3,9332E-13	-12,4053	0,0000	-12,4053
AlO2m	3,4770E-15	-14,4588	-0,1723	-14,6300	KOH(aq)	1,1007E-13	-12,9583	0,0000	-12,9583
NaAlO2	1,4560E-16	-15,8368	0,0000	-15,8400	AlO2-	3,5129E-15	-14,4543	-0,1556	-14,6099
H2SiO4	9,3790E-19	-18,0278	-0,7580	-18,7900	Al2(OH)2+++	1,1851E-15	-14,9263	-2,6791	-17,6054
Gas					Gas				
log(fugacity)					Log				
fugacity					Fugacity				
q0001 1,69E+00 4,91E+01					1,6907 4,91E+01				
Input File :					Elements Totals :				
Output file at t=102,11									
Ho	1,198671E-02			1,198671E-02	Ho	1,110285E+02			
Oo	2,212996E+00			2,212996E+00	Oo	5,772124E+01			
Alo	1,611574E-08			1,611574E-08	Alo	1,611574E-08			
Cao	1,074641E-02			1,074641E-02	Cao	1,074641E-02			
Clo	5,270593E-01			5,270593E-01	Clo	5,270593E-01			
Co	1,100383E+00			1,100383E+00	Co	1,100383E+00			
Ko	5,378551E-03			5,378551E-03	Ko	5,378551E-03			
Mgo	2,620624E-02			2,620624E-02	Mgo	2,620624E-02			
Nao	4,570086E-01			4,570086E-01	Nao	4,570086E-01			
So	1,052449E-05			1,052449E-05	So	1,052449E-05			
Sio	1,680689E-04			1,680689E-04	Sio	1,680689E-04			
H2Oo	5,550824E+01			5,550824E+01					

Construction of the coupled reaction-transport Usira simulator

The coupling of the geochemical UTSIRA simulator with the MARTHE flow and transport model is being initiated, according to a sequential non-iterative approach. It means that at each time step, for each cell, first hydrodynamics, then transport of each chemical component and finally chemistry (call of the geochemical UTSIRA simulator as an embedded subroutine) are calculated.

Conceived and developed by BRGM group for the hydrodynamic and hydrodispersive modelling of groundwater flow in porous media, the MARTHE software package is designed to resolve underground hydrodynamic problems in various contexts:

- Groundwater management
 - Groundwater balance assessment of aquifer systems : recharge by rainfall infiltration, groundwater flows and fluxes - inside the aquifer and exchanged through the aquifer boundaries -, yearly fluctuations, seasonal storages and withdrawals, ...
 - Hydrodynamic impacts of existing or planned works : pumping, irrigation, drainage, gravel extraction, infiltration basins, ...
 - Pumping/Wellfield management and optimization.
- Civil works
 - Dewatering of excavations.
 - Hydraulic effects of diaphragm walls.
 - Underground works (underground railways, car parks, tunnels, ...).
- Environment
 - Pollutant infiltration through the unsaturated zone down to the water table, then underground migration.
 - Modelling a pollutant plume originated from a contaminated zone : pathlines, velocities, concentrations. Comparison of various hydraulic schemes for containment or remediation.
 - Impacts on groundwater quality from municipal and industrial waste disposal facilities.
 - Containment study of underground storage facilities.
- Mining operations
 - Calculation of dewatering discharge and subsequent groundwater level drawdowns.

MARTHE can be used to simulate numerous types of groundwater flow, for saturated and unsaturated conditions, in monophasic and diphasic media. Five use levels are identified :

Level 1 :

- 2-D (plane level, vertical cross section, cylindrical coordinates) or 3-D grids.
- Single and multi-layer aquifers (aquifers sandwiched between aquitards).
- Unconfined, confined or semi-confined aquifers, in steady state or transient hydraulic conditions.
- Hydraulic discontinuities modelling, such as open bodies of water with free surface (lakes, gravel quarries, ...), local dewatering of aquifers (even for multi-layer aquifers), aquifer overflow (rivers, springs, drains, ...), diaphragm walls (sheet piles, ...).
- Horizontal and vertical permeability anisotropy.
- Calculation of pathlines (direct and reverse) in steady state or transient hydraulic conditions.

Level 2 :

- Dispersive migration of an effluent in an aquifer.

Level 3

- Continuous treatment of the saturated and unsaturated zones.
- Density effects caused by heterogeneous salinity and/or temperature fields.
- Variations in viscosity with temperature.

Level 4

- Automatic calibration of the model, according to homogeneous zones or cell by cell.
- Sensitivity analysis on calibration parameters.

Level 5

- Coupling with a river network and a drain network.
- Coupled hydroclimatic balance.
- Vertical conductive fractures modelled by equivalent transmissivities.
- Transport with physico-chemical interactions between water, effluents and porous matrix.
- Two-phase flow : water and air, water and "oil".
- Gas Flow.

The domain to be modelled is discretized as a rectangular "tartan" model : each row and each column of the grid has a constant width, but the user is free to adapt the width of each of these rows and columns so as to fit local heterogeneities, the amount of available data and the accuracy sought. It is also possible to create locally finer cells by nesting sub-grids.

The cells locations are automatically linked to geographic co-ordinates (SEMIS format created by BRGM group), enabling to superimpose the initial data and the results of simulations on previously digitized base maps. The data can be defined cell by cell, by zones, by layers or even for the whole grid. All the data are stored in ASCII text files.

The results of the modelling are produced in ASCII text files. They can be consulted with a text editor or plotted. The calculated flowrates (discharges in fixed head cells, residual discharges after convergence) can be presented cell by cell, by zones, by layers or for the whole grid.

The convergence of calculation is verified by several criteria : differences in head (average and maximum value between two successive iterations) and residual discharge after convergence (for the whole model, and locally in each of the cells).

The hydrodynamic flow calculations are carried out by a finite volumes algorithm. Several solutions are available, one of them based on a matrix resolution by conjugate gradients, with Choleski pre-conditioning.

The calculation of transport can be addressed through three calculations techniques, according to the type of problem encountered (predominance of convection or dispersion): (i) finite volumes method, (ii) method of characteristics (MOC) using particles, (iii) Random Walk method. Transport in the aquifer considers advective, diffusive and dispersive components, with two options being available: (i) exponential decrease of the effluent source as a function of time, (ii) retardation factor or partition coefficient, K_d (adsorption-desorption).

The physico-chemical interactions between water, effluents and rock matrix can be modelled by coupling MARTHE with a chemical model dedicated to the geochemical context (Thiéry, 1994; Kervévan *et al.*, 1998). The coupling scheme is iterative.

IFP MODELLING ACTIVITIES

In the framework of the SACS project, IFP is using the reaction-transport code DIAPHORE developed for the modelling of water-rock interactions, particularly those active during diagenesis of reservoirs. DIAPHORE can be used with a "box-system", closed or open. Alternatively, it can be used with a dimensional system. For modelling the lab experiments, the two options are used: the box system is adapted to the BGS batch experiments, and a 1-dimensional system was designed for simulating the GEUS coreflood experiments. The simulations presented here are preliminary tests to a significant comparison with the experiments, because at the date where this report is written only the batch experiments, launched three months ago, provided first results (water analyses).

In the lab experiments at 100 bars (10 MPa) and 37°C it is considered that the water is saturated with CO₂. As a consequence the DIAPHORE version used in SACS I calculates interactions occurring between the water phase (saturated in CO₂) and the chosen minerals. Another version of DIAPHORE is available, where it is possible to calculate the evolving composition of a gas phase at equilibrium with water (with extended Henry's law for the water-gas equilibrium and Peng-Robinson state equation for the gas). It was not used here.

Water composition, speciation and dissolved C calculations

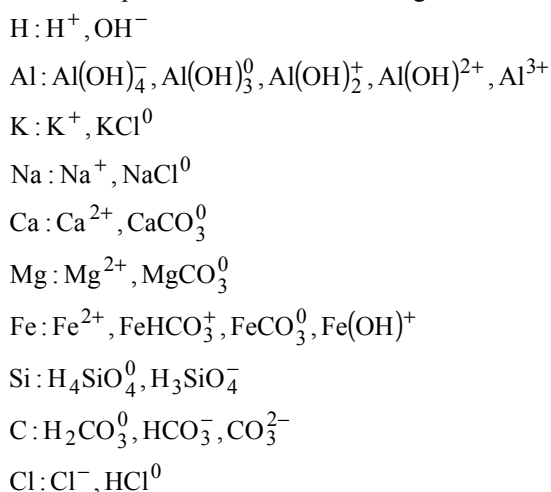
According to the Fig 6.5 of the Joule II Project N.CT92-0031 Final Report (Holloway *et al.*, 1996), the solubility of CO₂ in pure water at 37°C and 100 bars is approximately 55 g CO₂ / kg H₂O. According to Enick and Klara (1990) cited in the same report, in an aqueous solution with *ca* 3 wt.% of dissolved salts (*i.e.*, *ca* 30 g/l), the solubility is reduced to *ca* 85 % of this value, namely 47 g CO₂ / kg H₂O. This amount represents *ca* 0.94 mol C/ kg H₂O. This value was considered for running the following DIAPHORE simulations.

To the preceding value can be compared the experimental value provided by Takenouchi and Kennedy (1965) for a brine at 6 wt.% eq.NaCl, and 150°C, 100 bars : ca 2 wt.% CO₂ in the solution, *i.e.*, ca 0.45 mol C/ kg H₂O. It must be considered for the comparison that both temperature and salinity decrease the CO₂ solubility.

A calculation was made using the Soreide and Whitson's model (1992). It confirmed that the solubility in the considered conditions is approximately 1mol/kg water.

The synthetic Utsira porewater "SUP" was considered for running the DIAPHORE simulations (composition of the interstitial water initially present in the system, and of the water infiltrating the system in coreflood case). Its composition, as provided by the BGS (file from C. Rochelle, 10 Nov. 99), is reported as column 3 in Table 3.16 (molalities, *i.e.*, mol/kg H₂O). Sr, Ba, Mn, P, S, N and Br were not considered in the geochemical systems studied here. HCO₃ was reported as Total Inorganic Carbon (TIC).

For the simulations presented here the following elements and aqueous species were considered :



There is no redox reaction considered in this reported work.

For comparison purpose a speciation calculation was done for deciphering the natural conditions that normally prevail in an aquifer at a burial depth corresponding to 100 bars at a temperature of 37°C (column 2 in Table 3.16). The pCO₂ value was taken as 0.08 bar to be consistent with the Smith and Ehrenberg's pCO₂ vs T trend (1989), although this trend is poorly defined at temperature lower than 50°C. Al and Si were both fixed at 10⁻⁵ mol/kg H₂O. In such conditions the pH value is 6.6 and the total amount of dissolved C is ≈ 8.3 10⁻³ mol/kg H₂O. Such values can be compared : (a) to those of the Oseberg fluid analysis (column 1 in Table 1); (b) to those obtained for the CO₂-saturated water at fCO₂ = 35 bars (column 4 in Table 3.16).

Another calculation was made with fCO₂ = 55 bars and pH = 4.9. As shown by column 7 of Table 3.16, it resulted in lower chlorinity and higher C content than the preceding one.

Mineralogical system

A mineralogical composition was chosen from the Utsira sandstone composition analysed by BGS (Technical Report N. WG/99/24C by Pearce *et al.*, 1999). It is reported in Table 3.17 (column 1).

For the clay minerals the following compositions were chosen :

- illite : K_{0.8}(Si_{3.2}Al_{0.8})(Al_{1.9}Mg_{0.1}Fe_{0.1})O₁₀(OH)₂
- chlorite : (Si_{2.9}Al_{1.1})(Al_{1.7}Mg_{0.9}Fe_{3.1})O₁₀(OH)₈
- smectite (K-montmorillonite) : K_{0.3}(Si_{3.7}Al_{2.3})O₁₀(OH)₂

The thermodynamical constant for the hydrolysis reaction of these minerals was calculated according to the polyhedra method (Tardy and Garrels, 1974). The log K values provided by this method at 0, 25, 60, 100, 150, 200, 250 and 300°C are reported in Table 3.18. No correction was done for a pressure effect.

The characteristics of the minerals in terms of surface area, log K value at 37°C, and kinetic constant, are reported in Table 3.19. The kinetic rates were adjusted to match the values provided by BRGM during the last technical meeting (8 – 9 Nov. 99). The very large gap between kinetics of carbonates and silicates is worth being noted. The surface area offered by calcite was considered low because it was supposed that calcite is present in large-size biogenic debris (2 mm diameter) whereas detrital clastic grains (quartz, feldspars) have 100 µm "diameter" and clay minerals are 2 µm size crystallites. The DIAPHORE model computes the variations of grain size and surface areas according to a "floating sphere" model where the grains are assimilated to spheres of variable diameter.

Initial permeability was fixed at 2 darcys.

Simulations in closed system (to be compared to batch experiments)

Two simulations in closed system were made, the first one with water (4) of Table 3.16 ($f\text{CO}_2 = 35$ bars), the second one with water (7) of Table 3.16 ($f\text{CO}_2 = 55$ bars). Results after 1 and 2 years are reported in columns 5-6 (simul. N.1) and 8-9 (simul. N.2) of Table 3.16 (water) and Table 2 (minerals). The Figure 3.3 presents the evolution of total dissolved Ca obtained during 10 years throughout the second simulation.

The two simulations show a very similar result, *i.e.*, an extremely low interaction between water and the minerals. Approximately 1 % of the calcite present in the system dissolves in water (4), and 0.5 % in water (7). Nevertheless it seems that little variations in the pH / $f\text{CO}_2$ / chlorinity values could result in important changes of this proportion, or even in a reverse behaviour of calcite, *i.e.*, precipitation instead of dissolution ; this will have to be checked by additional simulations. Here, a situation that is probably near equilibrium is reached soon, before 1-year time.

A comparison can be made between these results and the first results obtained after 3-months batch experiment (information provided by BGS on the 9th of December 1999). In this experiment the Ca concentration in water goes from 432 ppm (0.011119 mol/kg.H₂O) to 1840 ppm (0.04762 mol/kg.H₂O) where it seems to have reached an equilibrium level (or at least a pseudo-equilibrium). The Ca value reached is very near the value obtained in the first simulation (Table 3.16, columns 5 and 6). In contrast, the value obtained in the second simulation (Table 3.16, columns 8 and 9) is lower. Moreover, the time at which Ca molality increases because of calcite dissolution is not accurate, it is too short compared to the 1-month time observed in the batch experiment. In future work matching the experiment will be a way to adjust the kinetics used in the simulation.

Interaction with alumino-silicates is extremely low at a few years time scale, what is normal considering the kinetic rates. The more visible trend concern the two feldspars, that begin to dissolve ($\approx 5 \cdot 10^{-3}$ % of their initial content in 2 years !). Dissolution of chlorite, and precipitation of quartz, concern even lesser quantities. K-montmorillonite (smectite) is inert.

Simulation in open, 1-dimensional system (for future comparison to coreflood experiments)

One simulation was made in an open system designed for representing the coreflood experiments : a 1-dimensional system 7.5 cm in length, 11.3569 cm² in section (GEUS document provided on 19 Nov.99). 50 grid elements of 1.5 mm length represent the system. The initial mineralogical composition and the porosity were kept equivalent to those used in the closed-system approach.

The simulation was made with a flow rate of $5.76 \cdot 10^{-6}$ m³/day (unit of DIAPHORE), *i.e.*, 0.24 ml/hr. This is 10 times the minimal flow rate indicated by GEUS. Considering the system size, with such a flow rate approximately 5 days and a half are needed to completely renew the interstitial water. During 1 year, approximately 70 water volumes infiltrate the sample. The water injected is the water (4) corresponding to $f\text{CO}_2 = 35$ bars (Tab. 3.16).

The main result of the simulation is the complete dissolution of calcite, that occurs as a reaction front crossing the system during the first year (Fig. 3.4 a, b). Before the front reaches the outlet, the Ca value in the part of the system where calcite is still present is very close to the concentration obtained in closed system for the test N.1 (compare column 11 to columns 5 or 6 in Table 3.16). Then it drops to the value imposed in the water infiltrating the system, because there is no more interaction with carbonates.

For the same reasons as previously mentioned, interaction with aluminosilicates is extremely low for the time intervals considered, due to the kinetic rates.

Table 3.16 Water compositions used for the DIAPHORE simulations.

Provided data are reported in columns 1 and 3. The other columns show compositions used as inputs or provided as outputs of the model. For this second set of columns the values imposed are noted in bold characters, and the values calculated by DIAPHORE in normal characters.

	1 Oseberg fluid analysis	2 Natural from SUP	3 Average SUP (BGS)	4 Initial + injected water bold : imposed	5 Closed system 1 year	6 Closed system 2 years	7 Initial water bold : imposed
pH	7.1	6.6	7.77	4.9	5.14	5.14	4.9
mol/kg H ₂ O :							
Na	0.466397	0.462458	0.462458	0.462458	0.463424	0.463454	0.462458
K	0.005489	0.005936	0.005936	0.005936	0.006002	0.006019	0.005936
Mg	0.026739	0.026862	0.026862	0.026862	0.026916	0.026917	0.026862
Ca	0.010967	0.011119	0.011119	0.011119	0.043084	0.043068	0.011119
Sr (10 ppm)							
Ba (0.5 ppm)							
Mn							
Fe	0.000037	0.000022	0.000022	0.000022	0.000022	0.000027	0.000022
Al		0.000010	< detect.	0.000010	0.000003	0.000001	0.000010
Si		0.000010	< detect.	0.000010	0.000163	0.000236	0.000010
P							
HCO ₃	0.011954	0.006295	see TIC	0.054966	0.064697	0.064711	
TOC							
TIC		0.008347	0.006526	0.934939	0.968774	0.968759	1.469170
Cl	0.537933	0.538034	0.542991	0.489439	0.490431	0.490431	0.458006
Br							
NO ₃							
SO ₄	n.d.						
fCO ₂ (bars)		0.08		35.0			55.0

Table 3.16 (continued)

	7 (repeat) Initial water (test 2) bold : imposed	8 Closed system 1 year	9 Closed system 2 years	4 (repeat) Initial + injected water bold : imposed	10 Open system 1 year inlet cell	11 Open system 1 year outlet cell	12 Open system 2 years outlet cell
pH	4.9			4.9			
mol/kg H ₂ O :							
Na	0.462458	0.463261	0.463268	0.462458	0.462458	0.463393	0.462459
K	0.005936	0.006052	0.006162	0.005936	0.005936	0.005950	0.005938
Mg	0.026862	0.026933	0.026943	0.026862	0.026862	0.026916	0.026862
Ca	0.011119	0.027073	0.027035	0.011119	0.011119	0.043106	0.011120
Sr							
Ba							
Mn							
Fe	0.000022	0.000104	0.000128	0.000022	0.000022	0.000022	0.000022
Al	0.000010	0.000003	0.000001	0.000010	0.000010	0.000013	0.000013
Si	0.000010	0.000132	0.000195	0.000010	0.000010	0.000017	0.000017
P							
HCO ₃				0.054966			
TOC							
TIC	1.469170	1.499170	1.499270	0.934939	0.934938	0.968790	0.934939
Cl	0.458006	0.458793	0.458792	0.489439	0.489440	0.490428	0.489440
Br							
NO ₃							
SO ₄							
fCO ₂ (bars)	55.0			35.0			

Table 3.17 Mineralogical compositions : initial state (column 1) ; evolved compositions, calculated by the DIAPHORE simulations (following columns).
Column numbers correspond to those already used in Table 3.16.

	1	5	6	8	9	10	11	12
	Initial compo- sition (Vol.%)	Closed system 1 year (Vol.%)	Closed system 2 years (Vol.%)	Closed system 1 year (Vol.%)	Closed system 2 years (Vol.%)	Open system 1 year (Vol.%) inlet cell	Open system 1 year (Vol.%) outlet cell	Open system 2 years (Vol.%) outlet cell
quartz	48.46	48.4600	48.4600	48.4600	48.4600	48.4600	48.4600	48.4600
K-feldspar	8.40	8.3997	8.3996	8.3996	8.3992	8.3995	8.3996	8.3991
albite	1.94	1.9399	1.9398	1.9400	1.9399	1.9399	1.9399	1.9398
calcite	3.88	3.8417	3.8417	3.8614	3.8615	< 10 ⁻⁶	3.8418	< 10 ⁻⁶
illite	0.65	0.6501	0.6501	0.6499	0.6496	0.6500	0.6500	0.6500
chlorite	0.65	0.6500	0.6500	0.6498	0.6498	0.6500	0.6500	0.6500
smectite	0.65	0.6500	0.6500	0.6500	0.6500	0.6500	0.6500	0.6500
porosity	35.37	35.4086	35.4088	35.3893	35.3899	39.2506	35.4087	39.2511

Table 3.18 Values of the log K calculated by the polyhedra method (Tardy and Garrels, 1974) for the three clay minerals considered in the simulations.

	0°C	25°C	60°C	100°C	150°C	200°C	250°C	300°C
illite	-54.603	-49.705	-45.001	-41.283	-38.105	-36.038	-34.846	-34.425
chlorite	-31.044	-30.581	-30.855	-31.542	-32.627	-33.944	-35.621	-37.817
smectite	-52.119	-48.191	-43.625	-39.304	-35.083	-31.443	-28.493	-26.814

Table 3.19 Characteristics used for the minerals in the DIAPHORE simulations.

The log K values are relative to the hydrolysis reaction expressed with the following aqueous species :

- H_2O and $H_4SiO_4^0$ for quartz ;
- $H_4SiO_4^0$, $Al(OH)_4^-$, Na^+ , K^+ , Ca^{2+} , Mg^{2+} , Fe^{2+} , H^+ (or H_2O) for aluminosilicates ;
- Ca^{2+} and CO_3^{2-} for calcite.

	log K at 37°C	Kinetic rate at 37°C mol/m ² .yr	Initial surface area m ² /l _{solution}
quartz	-3.803	3.45 10 ⁻⁶	6.3
K-feldspar	-22.170	1.145 10 ⁻⁴	1.1
albite	-19.340	2.88 10 ⁻⁵	0.25
calcite	-8.474	218	0.025
illite	-47.830	2.1 10 ⁻⁶	42.0
chlorite	-30.570	2.1 10 ⁻⁶	42.0
smectite	-46.510	22.1 10 ⁻⁶	42.0

Figure 3.3 Evolution of total dissolved Ca vs time in the closed-system simulation N.2 ($fCO_2 = 55$ bars). Compared to the batch experiment (first results available from BGS, the kinetics of calcite dissolution seems too rapid in the simulation (reactive surface area and / or kinetic rate), and the Ca molality reached after the reaction is too low (the value reached in simulation N.1 ($fCO_2 = 35$ bars) is better).

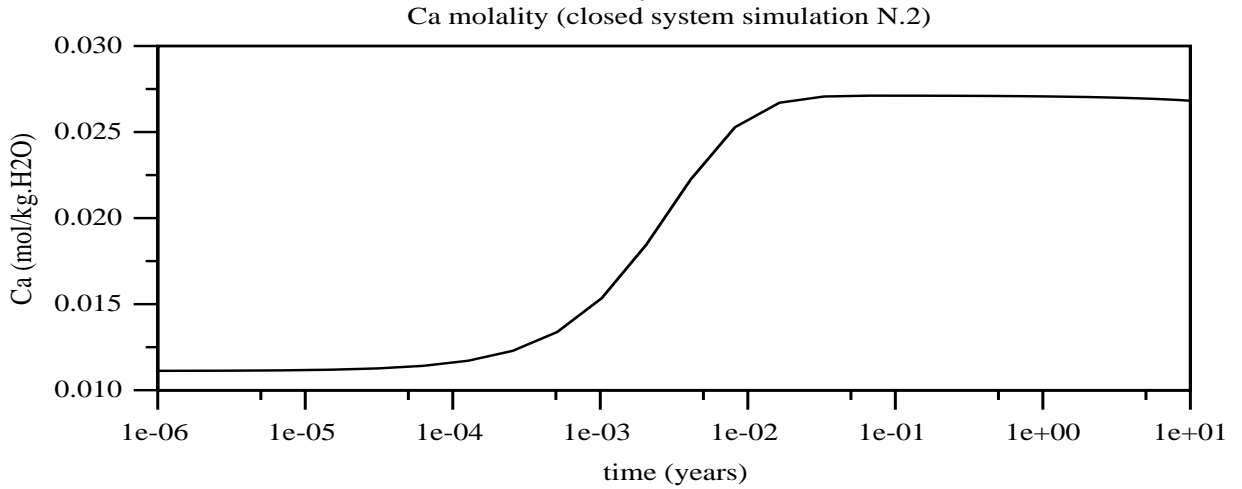


Figure 3.4a Evolution state of the open 1-dimensional system (coreflood experiment) simulated after 1 year at a flow rate of 0.24 ml/hr : a calcite dissolution front is located at 5 cm of the inlet.

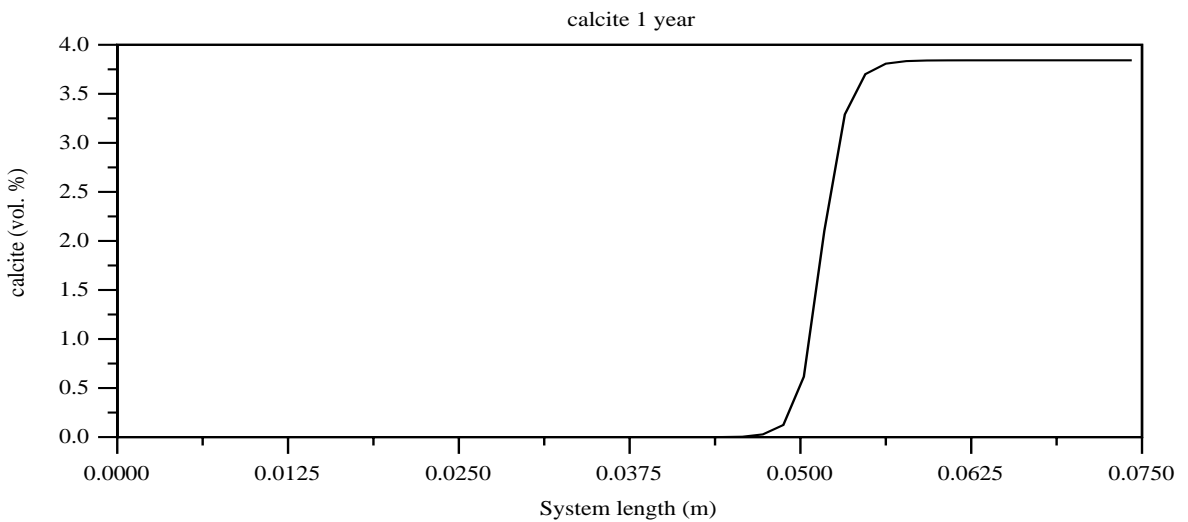
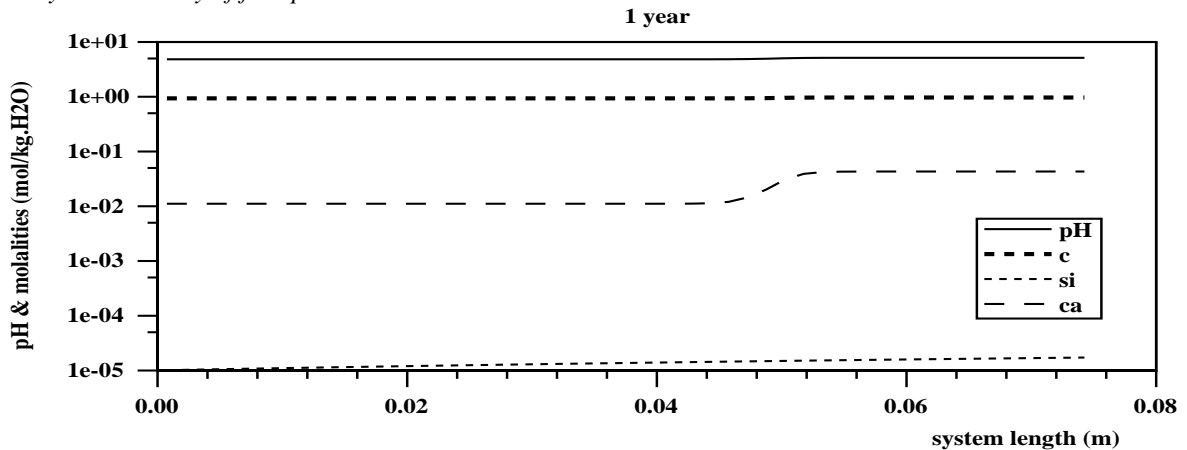


Figure 3.4b Evolution state of the open 1-dimensional system (coreflood experiment) simulated after 1 year at a flow rate of 0.24 ml/hr : pH, and molality of total C, Si and Ca.

The brutal decrease of the Ca content after the reaction front is due to the fact that there is no more calcite in the system, and the Ca value is similar to the Ca content of injected water. The Si evolution can be explained by the reactivity of feldspars.



3. Problems and difficulties encountered

WORK AREA 3. GEOCHEMISTRY

The main problem encountered during the reporting period was that of difficulties in obtaining rock and fluid samples, fluid chemical data and mineralogical data. This introduced some delay on the beginning of all tasks of the geochemical work programme, which was partly alleviated by the post-ponement of part of the work on the SACS II project.

In particular, Utsira formation fluid chemistry was very poorly constrained. Formation water was extracted from the frozen core and analytical results proved the core was heavily contaminated with drilling mud filtrate (Task 1.5). No mud sample was available to correct the formation brine data, and it is questionable if a correction was at all possible due to the substantial contamination.

The only available analysis was from the Oseberg field some 200 km from Sleipner (Gregersen *et al.*, 1998). In the absence of any other data, the Oseberg porewater composition had to be used as the starting point for the fluids used in the geochemical experiments. Synthetic equivalents were then made up. However, the reported Oseberg analysis contains no data for Al and Si, both of which are vital in order to establish the degree of saturation state of aluminosilicate minerals. Such minerals are very important as they have a major control on buffering solution pH (Czernichowski-Lauriol *et al.*, 1996; Gunter *et al.*, 1993; Hitchon, 1996; Hutcheon, 1993), and as a consequence, the ability of the porewater to dissolve CO₂.

The lack of firm data regarding baseline geochemistry is of broader importance than just for setting up the geochemical experiments. The uncertainties arising from the absence of such data may result in it being harder to defend the approaches taken in SACS when it comes to presenting the results of SACS to the public, regulatory bodies, and the scientific community.

A note has been written about the need to get at least a water sample and a caprock core sample in the Sleipner area, taking advantage of possible future exploratory wells.

At a more technical level, GEUS encountered difficulties with its new ICP-MS instrument which should be used in the project because it is considered as an advantage to run all elements (except Na) on the same instrument. However, a number of technical problems occurred with this instrument in the beginning, and it was early October before we had the first usable results. Finally in late November Si could also be analyzed, but the analytical programme for the project was delayed for some months.

IFP reported some difficulties for calculating fCO₂, due to the DIAPHORE version used. The gas version will be used in SACS II.

4. Any changes or modifications from the original project

WORK AREA 3: GEOCHEMISTRY

The original project description envisaged the probable need for experiments to determine the rates of reaction of certain key minerals. However, it soon became apparent that determination of pH within the experiments was of much higher priority. Therefore, any effort aimed originally at supporting mineral kinetics determination was switched to pH determination.

The original project description was aimed at equal emphasis being placed on caprock batch experiments and Utsira sand batch experiments. Unfortunately, intact core samples of caprock were not available. Therefore, only a few experiments using cleaned drill chippings of caprock will be conducted, but a larger number of experiments using the Utsira sand will be performed.

The GEUS original idea of conducting the flow experiments in a closed system mode, ie. by recirculating a fixed amount of fluid through the samples, was abandoned because it was very similar to the batch experiments. It is

now decided to conduct open system experiments, ie. fresh formation brine will be flooded through the samples continuously to secure maximum reaction with the minerals in the Utsira sand.

5. Compliance with the work programme as outlined in Annex I

WORK AREA 3: GEOCHEMISTRY

In general, work is proceeding broadly in line with the work programme. However, there were some delays caused by lack of rock material, fluid and mineralogical data. These delays should not affect the overall experimental programme, as part of the work was post-poned on SACS II.

6. Cost variations from the given original estimate included in the contract

WORK AREA 3: GEOCHEMISTRY

Cost variations were due to the decision of the Steering Committee meeting to acquire seismic data in 1999.

The overall cost of the BGS experimental work programme within SACS I and SACS II has remained unchanged. However, the relative split of costs between then has changed, with a reduction of costs in SACS I and an increase in SACS II. The original cost estimate in SACS I was approximately 101k Euro, but was reduced to approximately 71k Euro. The original cost estimates for years 1 and 2 of SACS II were approximately 29k Euro and 14k Euro respectively, which are now increased to approximately 37k Euro for both.

The overall cost of the BRGM geochemical work programme within SACS I and SACS II has remained unchanged. However, the relative split of costs between then has changed, with a reduction of costs in SACS I and an increase in SACS II. The original cost estimate in SACS I was 62k Euro, but was reduced to 52k Euro. The original cost estimates in SACS II was 28k Euro, which is now increased to 37k Euro.

The overall cost of the IFP geochemical work programme within SACS I and SACS II has remained unchanged. However, the relative split of costs between then has changed, with a reduction of costs in SACS I and an increase in SACS II. The original cost estimate in SACS I was 36k Euro, but was reduced to 26k Euro. The original cost estimates in SACS II was 31k Euro, which is now increased to 40k Euro.

The GEUS original budget for geochemistry in SACS I was 101k Euro, but this has been cut to approx. 85k Euro. The cost estimates for SACS II, year 1 and 2, remains at 29k and 14k EURO respectively.

7. Patents, if any, applied for or issued during the reporting period

No patents were applied for or issued during the reporting period.

8. Brief forecast of the next six month's activities and work

WORK AREA 3 - GEOCHEMISTRY

TASK 3.1. DETERMINATION OF THE INITIAL FLUID/ROCK EQUILIBRIUM IN UTSIRA FORM (BRGM)

Further calculations will be carried out within SACS II and refinements will be achieved working on thermodynamic data, mineralogical observations and results of the blank experiments. The latter will be of great interest for studying the baseline geochemistry before CO₂ injection.

TASK 3.2. GEOCHEMICAL LABORATORY EXPERIMENTS

BGS

Long term, long pathlength flow experiments

These experiments should start early in SACS II. They are aimed at providing the geochemical modelling groups with 'test cases' with which to 'benchmark' the various modelling packages being employed in SACS. Two experiments are envisaged, both to run at 70 °C and 10 MPa, and have a duration of about 12 months.

The first experiment will use Utsira sand and synthetic Oseberg porewater saturated with CO₂. The sand will be packed into a rigid column of 0.7 cm diameter and 240 cm length. This experiment will have the benefits of being relatively simple and having directly comparable mineralogy to that at Sleipner. However, there will be no confining pressure, just 10 MPa of porewater pressure. Fluid sampling will be once or twice a week, and so will necessitate a minimum flow rate of about 30-40 ml/week. However, the final choice of flow rate will depend upon data from the batch experiments (see Task 3.2 report above). The column will be into sections for mineralogical analysis after the experiment. A report will be produced that describes changes in output fluid chemistry and mineralogy, together with a preliminary interpretation.

The second experiment will use a synthetic representation of the Utsira formation made up from precisely-known quantities of pure mineral phases. These will be packed into a flexible metal or 'plastic' tube of approximately 2.5 cm diameter and 100 cm length. Although this experiment will not use actual Utsira sand, it will have the benefit of being a 'half way house' that will hopefully provide the modelling groups with a relatively simple test case to use in their modelling. 10 MPa of porewater pressure will be applied again, with its composition made according to the saturation of the minerals concerned at the experimental temperature. Fluid sampling will be once or twice a week, and so will necessitate a minimum flow rate of about 30-40 ml/week. However, the final choice of flow rate will depend upon data from the column experiment above and from the batch experiments (see Task 3.2 report above). The 'sand pack' will be into sections for mineralogical analysis after the experiment. A report will be produced that describes changes in output fluid chemistry and mineralogy, together with a preliminary interpretation.

Long term batch experiments at a temperature above in-situ conditions

These experiments should start early in SACS II. They will be very similar to the batch experiments described in Section 2.1 above, except for their higher temperature. It is often possible to trade off temperature for time in experimental studies, and an approximate doubling of temperature (from the 37 °C of those in Task 3.2 above, to 70 °C) can increase reaction rate by a factor of 10 - 15. As a consequence, it is therefore possible to investigate slow reactions over a much shorter timescale.

pH measurement

Development of this technique will continue into SACS II, and it is envisaged that this will become a standard analytical technique applied when sampling any experiment.

GEUS

The blind experiment running for the 3 preserved core samples will continue till January 2000. The experiment will then shift to synthetic Utsira formation water saturated with CO₂ and run for 1-2 months. A tracer study will be conducted using the final preserved core plug. Following experiments will rely on sandpicks because it is no longer possible to take preserved (frozen) core plugs from the 0.9 meter section of full core received for the study. Later experiments will be conducted at elevated temperature of 70 °C to speed reaction rates. After experiment the core plugs will be cut into sections and analyzed mineralogically.

TASK 3.3. INTERPRET LABORATORY EXPERIMENTS

BRGM, IFP: Progressive integration of the results coming from the experiments.

9. REFERENCES

- AJA S.U., 1995. Thermodynamic properties of some 2:1 layer clay minerals from solution-equilibration data. *Eur. J. Mineral.*, 7, 325-333.
- AZAROUAL M., KERVEVAN C. and GIRARD J.P., 1999. SCALESIM for PC – User's manual, *BRGM Report n° R 40502*, 20 p.
- BILDSTEIN, O., 1998. Modélisation géochimique des interactions eau-gaz-roche. Ph.D IFP–Strasbourg University, 227 p.
- CZERNICHOWSKI-LAURIOL, I., SANJUAN, B., ROCHELLE, C., BATEMAN, K., PEARCE, J. and BLACKWELL, P. 1996. Inorganic geochemistry. Chapter 7 in *'The Underground Disposal of Carbon Dioxide'* (S. Holloway ed.), Final Report of Joule II Project Number CT92-.
- DRUMMOND S.E. Jr., 1981. Boiling and mixing of hydrothermal fluids: Chemical effects on mineral precipitation, Pennsylvania State University, Unpublished Ph. D. Thesis. In SOLMINEQ.88: A computer program for geochemical modelling of water-rock interactions by Kharaka et al., 1988, 420 p.
- EGEBERG P.K. and AAGAARD P., 1989. Origin and evolution of formation waters from oil fields on the Norwegian shelf. *Appl. Geochem.*, 4, 131-142.
- ELLIS, A. J. & GOLDING, R. M. 1963. The solubility of carbon dioxide above 100°C in water and in sodium chloride solutions. *American Journal of Science*, 261, 47-60.
- ENICK, R.M. and KLARA, S.M., 1990. CO₂ solubility in water and brine under reservoir conditions. *Chem. Eng. Comm.*, Vol. 90, pp. 23-33.
- HELGESON H.C, 1969. Thermodynamic of hydrothermal systems at elevated temperatures and pressures. *American Journal of Science*, 267, 729-804.
- HOLLOWAY *et al* (1996).- *The underground disposal of carbon dioxide*. Final Report of the Joule II Project NO. CT92-0031, 355 p.
- GREGERSEN, U., JOHANNESSEN, P. N., MILLER, J. J., KRISTENSEN, L., CHRISTENSEN, N. P., HOLLOWAY, S., CHADWICK, A., KIRBY, G., LINDEBERG, E. and ZWEIGEL, P. 1998. Saline Aquifer CO₂ Storage (S.A.C.S.) Phase Zero 1998 report.
- GUNTER, W. D., PERKINS, E. H. and MCCANN, T. J. 1993. Aquifer disposal of CO₂-rich gases: reaction design for added capacity. *Energy Conversion Management*, 34, 941-948.
- GUNTER, W. D., WIWCHAR, B. & PERKINS, E. H. 1997. Aquifer disposal of CO₂-rich greenhouse gases: extension of the time scale of experiment for CO₂-sequestering reactions by geochemical modelling. *Mineralogy and Petrology*, 59, 121-140.
- HITCHON, B. (ed.) 1996. *Aquifer Disposal of Carbon Dioxide, Hydrodynamic and Mineral Trapping - Proof of Concept*. Geoscience Publishing Ltd, Alberta, Canada, 165p.
- HUTCHEON, I., SHEVALIER, M. & ABERCROMBIE, H. J. 1993. pH buffering by metastable mineral-fluid equilibria and evolution of carbon dioxide fugacity during burial diagenesis. *Geochimica et Cosmochimica Acta*, 57, 1017-1027.
- JOHNSON J.W., OELKERS E.H. and HELGESON H.C., 1992. SUPCRT92: A software package for calculating the standard molal thermodynamic properties of minerals, gases, aqueous species and reactions from 1 to 5000 bar and 0 to 1000°C. *Computers and Geosciences*, 18, 899-947.

- KERVEVAN C., BARANGER P., 1998. SCS : Specific Chemical Simulators dedicated to chemistry-transport modelling. Part I – Design and construction of an SCS. Goldschmidt Conference, Toulouse, 29th August-3rd September, in : *Min. Magazine*, (62A), 771-772.
- KERVEVAN C., THIERY D., BARANGER P., 1998. SCS : Specific Chemical Simulators dedicated to chemistry-transport modelling. Part III – Coupling of SCS with the hydro-transport modelling software MARTHE. Goldschmidt Conference, Toulouse, 29th August-3rd September, in : *Min. Magazine*, (62A), 773-774.
- KHARAKA Y.K., HULL R.W. and CAROTHERS W., 1985. Water-rock interaction in sedimentary basins. In relationship of Organic Matter and Mineral Diagenesis (Eds D.L. Gauthier, Y.K. Kharaka and R.C. Surdam). *Soc. Econ. Paleont. Mineral.*, 17, 79-174.
- MICHARD G., 1983. Recueil de données thermodynamiques concernant les équilibres eaux-minéraux dans les réservoirs hydrothermaux. *CCE Report EUR 8590FR*.
- NORDSTROM D.K., PLUMMER L.N, WIGLEY T.M.L., WOLERY T.J, BALL J.W., JENNE E.A., BASSETT R.L., CRERAR D.A., FLORENCE T.M., FRITZ B., HOFFMAN M., HOLDREN G.R. JR, LAFON G.M., MATTIGOD S.V., MCDUFF R.E., MOREL F., REDDY M.M., SPOSITO G. and THRAILKILL J., 1979. A comparison of computerized chemical models for equilibrium calculations in aqueous system. In Jenne, E.A, editor, *Chemical Modeling in Aqueous Systems, American Chemical Society Symposium Series*, v.93, American Chemical Society, Washington, D.C., 857-892.
- PEARCE, J.M., KEMP, S.J. and WETTON, P.D., 1999. Mineralogical and petrographical characterisation of a 1 m core from the Utsira formation, Central North Sea. *BGS Report No. WG/99/24C* of the SACS Project, 16 p.
- ROBIE R.A., HEMINGWAY B.S. and FISHER J.R., 1978. Thermodynamic properties of minerals and related substances at 298.15°K and 1 bar (10^5 Pascal) pressure and at higher temperatures. *U.S. Geol. Survey Bull.* 1452, 456 p.
- SANJUAN B., GIRARD J.P. and CZERNICHOWSKI I., 1995. Geochemical modelling of the main diagenetic processes in the Oseberg sandstone reservoir, Oseberg field, northern North Sea. *BRGM report R38599*, 167 p.
- SANJUAN B., GIRARD J.P., LANINI S., BOURGUIGNON A. and BARITEAU A., 1999. Geochemical modelling of diagenetic illite formation in the Brent Group sandstones, Hild oil field (Norwegian North Sea). In: CEC DIAMAP project final report, in press.
- SOREIDE, I. and WHITSON, C.H., 1992. Peng-Robinson predictions for hydrocarbons, CO₂, N₂, and H₂S with pure water and NaCl brine. *Fluid Phase Eq.*, 77, pp. 217-240.
- STEWART, P. B. and MUNJAL, P. K. 1970. The solubility of carbon dioxide in pure water, synthetic sea water and synthetic sea-water concentrates at -5 to 25 °C and 10 to 45 atm pressure. *Journal of Chemical and Engineering data*, 1591, 67-71.
- TAKENOUCHI, S. and KENNEDY, G.C., 1965. The solubility of carbon dioxide in NaCl solutions at high temperatures and pressures. *Am. J. of Sci.*, Vol. 263, pp. 445-454.
- TARDY Y. and DUPLAY J., 1992. A method of estimating the Gibbs free energies of formation of hydrated and dehydrated clay minerals. *Geochim. Cosmochim. Acta*, 56, 3007-3029.
- TARDY, Y. and GARRELS, R.M., 1974. A method for estimating the Gibbs energies of formation of layer silicates. *Geochem. Cosmochem. Acta*, Vol.56, pp. 1101-1116.
- THIERY D., 1990. Modélisation des écoulements avec interactions chimiques avec le logiciel MARTHE version 5.5. *BRGM Report n° R38463*, 200 p.
- THIERY D., 1994. Logiciel MARTHE version 4.3. *BRGM Report n° R32210*, 200 p.
- TOEWS, K. L., SHROLL, R. M. and WAI, C. M. 1995. pH-defining equilibrium between water and supercritical CO₂. Influence on SFE of organics and metal chelates. *Analytical Chemistry*, 67, 4040-4043.
- WOLERY T.J., 1992. EQ3/6 : A Software Package for Geochemical Modeling of Aqueous Systems : Package Overview and Installation Guide (version 7.0), Lawrence Livermore National Laboratory, Report UCRL-MA-110662 PT I, California, USA

WOLERY T.J., 1995. EQ3/6, a software package for geochemical modeling of aqueous systems: package overview and installation guide (version 7.2b). Lawrence Livermore National Laboratory, Livermore, California.